AD_____

Award Number: DAMD17-03-1-0231

TITLE: Targeting Stat3 with G-quartet Oligonucleotides in Metastatic Prostate Cancer

PRINCIPAL INVESTIGATOR: Naijie Jing, Ph.D.

CONTRACTING ORGANIZATION: Baylor College of Medicine
Houston, TX 77030

REPORT DATE: April 2004

TYPE OF REPORT: Annual

PREPARED FOR: U.S. Army Medical Research and Materiel Command
Fort Detrick, Maryland 21702-5012

REPORT DOCUMENTATION PAGE

Form Approved OMB No. 074-0188

1. AGENCY USE ONLY (Leave blank)	2. REPORT DATE	3. REPORT TYPE AND DATES COVERED
	April 2004	Annual (1 Apr 2003 - 31 Mar 2004)

4. TITLE AND SUBTITLE

Targeting Stat3 with G-quartet Oligonucleotides in Metastatic Prostate Cancer

5. FUNDING NUMBERS

DAMD17-03-1-0231

6. AUTHOR(S)

Naijie Jing, Ph.D.

7. PERFORMING ORGANIZATION NAME(S) AND ADDRESS(ES)

Baylor College of Medicine
Houston, TX 77030

E-Mail: njing@bcm.tmc.edu

8. PERFORMING ORGANIZATION REPORT NUMBER

9. SPONSORING / MONITORING AGENCY NAME(S) AND ADDRESS(ES)

U.S. Army Medical Research and Materiel Command
Fort Detrick, Maryland 21702-5012

10. SPONSORING / MONITORING AGENCY REPORT NUMBER

11. SUPPLEMENTARY NOTES

Original contains color plates: ALL DTIC reproductions will be in black and white

12a. DISTRIBUTION / AVAILABILITY STATEMENT

Approved for Public Release; Distribution Unlimited

12b. DISTRIBUTION CODE

13. ABSTRACT (Maximum 200 Words)

This annual report is composed of (1) introduction of the goal of this project and specific aims, (2) research accomplishments by PI group from 4/1/03/ to 3/31/04 including one publication and one manuscript, (3) summary of results and significance, and (4) conclusion of the project studies. This report demonstrated that during the period from 4/1/03 to 3/31/04, PI group made a significant progress in developing a novel and potent anti-cancer agent, which holds promise or the systemic treatment of prostate cancer.

14. SUBJECT TERMS

G-quartet oligonucleotides; Stat3; Prostate cancer; Rational drug design; Anti-cancer agent

15. NUMBER OF PAGES

51

16. PRICE CODE

17. SECURITY CLASSIFICATION OF REPORT	18. SECURITY CLASSIFICATION OF THIS PAGE	19. SECURITY CLASSIFICATION OF ABSTRACT	20. LIMITATION OF ABSTRACT
Unclassified	Unclassified	Unclassified	Unlimited

Annual Report 1 for Award: PC020407

Naijie Jing, Ph. D
Assistant Professor
Department of Medicine/Infectious Diseases
Baylor College of Medicine
One Baylor Plaza, N1319
Houston, TX 77030
Tel: 713-798-3685
Fax: 713-798-8948
E-mail: njing@bcm.tmc.edu

Table of Contents

Appendices:

1. Jing, N., Li, Y., Xcu, X., Li, P., Feng, L., Tweardy, D. "Inhibitor of Stat3 Activity by G-quartet oligodeoxynucleotides in human cancer cells" (2002) *DNA and Cell Biology* (2003) 22, 685-696.
2. Naijie Jing, Li, Y., Xiong, W., Sha, W. Jing, L. Tweardy, D. J. "G-quartet oligonucleotides: a new class of Stat3 inhibitors that suppresses growth of prostate and breast tumors through induction of apoptosis" submitted (2004).

I. Introduction.

Our goal is to develop a novel, potent inhibitor of Stat3 as a therapeutic drug for suppressing the growth of prostate cancer. Prostate cancer is a major public health problem in United States and worldwide and is the second most common cause of cancer deaths in North American men. In the year 2003, carcinoma of the prostate accounted for an estimated 220,900 new cancer cases and 28,900 deaths. Currently, chemotherapy is not very successful in prostate cancer. Mounting evidence from cell culture, whole animals and patient samples demonstrate that Stat3 is a critical mediator of oncogenic signaling and is active in 82% of prostate cancers, 69% of breast cancers, 82-100% of head and neck cancers (HNSCC), 71% of nasopharygeal carcinoma as well as in many other cancers. However, Stat3 has been little targeted with current chemotherapeutic approaches. Developing a novel and promising treatment for prostate cancer will be greatly helpful both in terms of single agent treatment and as part of a combination therapy. The Specific Aims designed to achieve this objective are outlined as below

Specific Aim 1: To develop a potent inhibitor of Stat3 to suppress growth of prostate cancer cells in cell culture.
Specific Aim 2: To develop an effective delivery system and to test the inhibition of growth of prostate tumors for our designed inhibitors *in vivo*.

II. Research Accomplishments by PI group from 4/1/03 to 3/31/04.

Publications:
1. Targeting Stat3 with G-quartet oligodeoxynucleotides in human cancer cells. (Jing et al. *DNA and Cell Biology* 22, 685-696 (2003)).
ABSTRACT: Stat3 is an oncogene that is activated in many human cancer cells. Genetic approaches that disrupt Stat3 activity result in inhibition of cancer cell growth and enhanced cell apoptosis supporting the development of novel drugs targeting Stat3 for cancer therapy. G-quartet oligodeoxynucleotides (ODNs) were demonstrated to be potent inhibitors of Stat3 DNA binding activity *in vitro* with the G-quartet ODN, T40214, having an IC_{50} of 7 μM. Computer-simulated docking studies indicated that G-quartet ODNs mainly interacted with the SH2 domain of Stat3 and were capable of inserting between the SH2 domains of Stat3 dimers bound to DNA. We demonstrated that the G-rich ODN T40214, which forms a G-quartet structure at intracellular but not extracellular K^+ ion concentrations, is delivered efficiently into the cytoplasm and nucleus of cancer cells where it inhibited IL-6-stimulated Stat3 activation and suppressed Stat3-mediated up-regulation of *bcl-x* and *mcl-1* gene expression. Thus, G-quartet represents a new class of drug for targeting of Stat3 within cancer cells.

2. G-quartet oligonucleotides: a new class of Stat3 inhibitors that suppresses growth of prostate and breast tumors through induction of apoptosis. (Jing et al. submitted (2004)).
ABSTRACT: Stat3 is a signaling molecular and oncogene activated frequently in many human malignancies including the majority of prostate, breast and head and neck cancers; yet, no current chemotherapeutic approach has been implemented clinically that specifically targets Stat3. We recently developed G-rich oligodeoxynucleotides, which form intramolecular G-quartet structures (GQ-ODN), as a new class of Stat3 inhibitor. GQ-ODN targeted Stat3 protein directly inhibiting its ability to bind DNA. When delivered into cells using polyethyleneimine (PEI) as vehicle, GQ-ODN blocked ligand-induced Stat3 activation and Stat3-mediated transcription of anti-apoptotic genes. To establish the effectiveness of GQ-ODN as a potential new chemotherapeutic agent, we systemically

administered GQ-ODN plus PEI or PEI alone (placebo) by tail vein injection into nude mice with prostate and breast tumor xenografts. While the mean volume of breast tumor xenografts in placebo-treated mice increased by 6.7 fold over 18 days, xenografts in the GQ-ODN-treated mice remained unchanged (p=0.006). Similarly, while the mean volume of prostate tumor xenografts in placebo-treated mice increased 9 fold over 10 days, xenografts in GQ-ODN-treated mice increased by only 2.2 fold (p=0.001). Biochemical and histological examination of tumors from mice treated with G-quartet ODN demonstrated a 9-fold reduction in Stat3 activation, a reduction in levels of the anti-apoptotic proteins Bcl-2 and Bcl-x_L of 4 fold and 10 fold, respectively, and a 8-fold increase in the number of apoptotic cells compared to the tumors of placebo-treated mice. Thus, GQ-ODN targeting Stat3 induce tumor cell apoptosis when delivered into tumor xenografts following intravenous injection and represent a novel class of chemotherapeutic agents that holds promise for the systemic treatment of many forms of metastatic cancer.

Presentations in Scientific Conferences:

1. 94th AACR Annual meeting, 7/11-14/2003, Washington, DC.
Title: G-quartet Oligodeoxynucleotides: a potent inhibitor of Stat3 for cancer therapy.
ABSTRACT: Signal transducer and activator of transcription (Stat) 3 is an oncogene that is activated in many human cancer cells. Genetic approaches that disrupt Stat3 activity within cancer cells result in inhibition of cell growth and enhanced cell apoptosis, supporting the development of novel drugs targeting Stat3 for cancer therapy. Our newly designed G-quartet oligodeoxynucleotide (ODN), T40214, has been effectively delivered into human cancer cells where it significantly inhibited Stat3 activation (IC50 = 7μM) and suppressed the expression of Stat3-regulated genes, *bcl-x*. Computer-based docking analysis predicted that inhibition of Stat3 by the G-quartet ODN occurred mainly through its interaction with the SH2 domains of Stat3 homodimers. The results of *in vivo* delivery demonstrated that T40214 was well distributed within many critical tissues, such as breast and prostate gland, showing a promising future for treatment of metastatic human cancers. Our drug tests on nude mice with prostate tumor xenograft demonstrated that T40214 as a potent Stat3 inhibitor suppressed the growth of prostate tumors.

2. AACR-NCI-EORTC International Conference—Molecular Target and Cancer Therapeutics, 11/17-21/2003, Boston, MA.
Title: G-quartet ODNs as a novel Stat3 inhibitor suppress the growth of breast and prostate tumors.
ABSTRACT: Stat3 is an oncogene activated in many human cancer cells. Genetic approaches that disrupt Stat3 activity result in inhibition of cancer cell growth and enhanced cell apoptosis supporting the development of novel drugs targeting Stat3 for cancer therapy. G-quartet oligodeoxynucleotides (ODNs) were demonstrated to be potent inhibitors of Stat3 DNA binding activity *in vitro* with the G-quartet ODN, T40214, having an IC_{50} of 7 μM. Computer-simulated docking studies indicated that G-quartet ODNs mainly interacted with the SH2 domains of Stat3 dimer and were capable of inserting between the SH2 domains to destabilize the dimer formation. Using polyethyleneimine (PEI) as a carrier, we demonstrated that the G-rich ODN T40214, which forms a G-quartet structure at intracellular but not extracellular K^+ ion concentrations, was delivered efficiently into the cytoplasm and nucleus of cancer cells where it inhibited IL-6-stimulated Stat3 activation and suppressed Stat3-mediated up-regulation of *bcl-x* and *mcl-1* gene expression. Microscopic examination of mice 24 hr following intravenous administration of PEI complexes containing fluorescein-labeled T40214 demonstrated diffuse fluorescent staining of T40214 in all organs (liver, kidney, breast, prostate gland) as well as human prostate and breast cancer xenografts from animals. To assess if tumor uptake is accompanied by inhibition of tumor growth, mice were injected subcutaneously with human prostate tumor cells (PC-3) or breast (MDA-MB-468), both of which demonstrate constitutive Stat3

activity. One group received T40214 (5.0 mg/kg) plus the vehicle (PEI, 2.5 mg/kg), the other group (placebo) received PEI (2.5 mg/kg) alone intravenously every other day starting after the tumors were established. The results demonstrated that the mean size of breast tumors of placebo-treated mice increased by 6.7 fold while tumors of drug-treated mice remained unchanged (p=0.006). The prostate tumors of placebo-treated mice increased 9.3 fold while tumor in drug-treated mice increased by only 2.2 fold (p=0.003). Prostate tumors from 3 placebo-treated mice and 4 drug-treated mice were harvested after the preriod of treatment and then assessed for number of apoptotic cells by TUNEL and protein extracted for immunoblotting to assess for levels of Stat3 protein phosphorylated on Y705 and levels of Bcl-x_L protein and activated caspase 3. Levels of phosphorylated Stat3 (p-Stat3) were decreased 9-fold (P=0.004), Bcl-x_L levels were decreased 4-fold (P<0.001) while caspase 3 cleavage products were increased about 3-fold in the tumors from drug-treated animals compared to tumors from placebo-treated mice. TUNEL assay demonstrated a 6-fold increase in apoptotic cells in the tumors of drug-treated mice compared to tumors of placebo-treated mice. Thus, T40214 suppressed the growth of breast and prostate tumors by inhibiting Stat3 activation, resulting in a dramatic enhancement of tumor cell apoptosis. Thus, G-quartet ODNs represent a novel class of Stat3 inhibitors that shows promising agent for cancer therapy in tumors with constitutive Stat3 activity.

III. Summary of results and significance.

1. Mechanism of GQ-ODN as an inhibitor of Stat3.

Based upon our recent results, we modeled the inhibition of Stat3 by GQ-ODNs as shown in Figure 1. Monomers of Stat3 in the cytoplasm of unstimulated cells become activated by cytokine or growth factor receptor, including IL-6, EGFR and other cytokine, binds to its cognate receptors on the cell surface. Tyrosine phosphorylation of Stat3 induces formation of active Stat3 dimers via its SH2 domains, recruited by intrinsic or receptor-associated tyrosine kinases such as JAK. Then the activated Stat3 dimers translocate to the nucleus, where they bind to DNA-response elements in the promoters of target genes and activate specific gene expression programs. GQ-ODNs are delivered into the cytoplasm by PEI/DNA complexes. Induced by the elevated K^+ concentration within the cytoplasm, ODNs form G-quartet structures, which diffuse into the nucleus and inhibit the activation of phosphorylated Stat3. The inhibition of Stat3 activation decreases expression of Stat3-regulated genes, notably those encoding anti-apoptosis proteins, such as Bcl-x_L, Bcl-2 and Mcl-1, which reduces their levels below a critical threshold and triggers cell apoptosis.

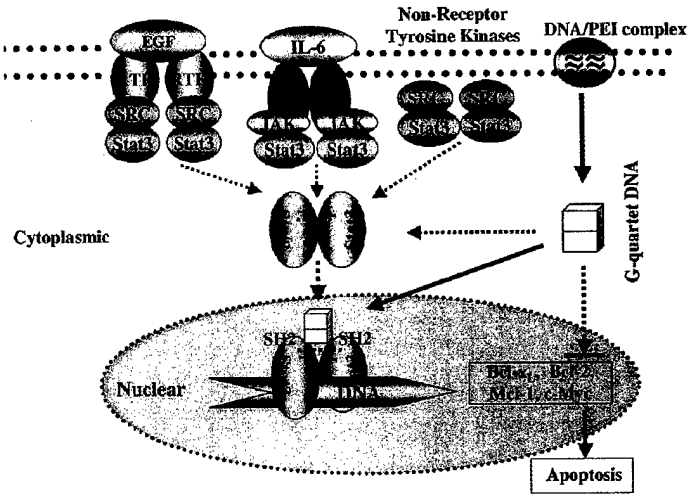

Figure 1. Mechanism of inhibition of Stat3 by GQ-ODNs.

2 Rational drug design of GQ-ODNs as an anti-cancer agent.

Our drug design system is based upon two assumptions: (i) The structure of the target molecule contains a reasonable molecular shape of the binding site, and (ii) the structure of inhibitor/target molecule complex obtained from docking is a useful starting point for searching for an effective inhibitor. To construct a drug design system, we employed a statistical docking system using GRAMM and randomly docked the known structure of GQ-ODN into the crystal structure of Stat3β

dimer one or two thousand times without setting binding site restrictions. The results of the statistical docking demonstrated the probability of interaction between drug and target molecules, identified the potential binding sites on the target molecule and established a structure of GQ-ODN/Stat3β dimer complex for our structure-based drug design (Appendix 1). A rational drug design system can make a backup rapidly available when a candidate is found to have inadequate drug properties in clinical trials.

Structure-activity relationship (SAR) has proven to be extremely useful in the design of biologically active molecules. SAR correlates the relative biological potency of inhibitors with their physical properties. Establishing a specific SAR is a key step for our drug design system. A linear SAR was recently established that directly correlated the ability of a GQ-ODN to bind to a region within the Stat3 SH2 domain, which is critical for dimerization, with its ability to inhibit Stat3 activity within cells (Appendix 2). The correlation indicated that the higher the percentage of GQ-ODN H-bond formation within this region of Stat3 SH2, the greater its ability to inhibit Stat3 activation within cells, which is an important step towards optimizing the design of GQ-ODN inhibitors of Stat3.

3. Advantages of GQ-ODNs as an anti-cancer agent.

(1). We have constructed a model of GQ-ODN/Stat3 complex and established a structure-activity relationship (SAR) between GQ-ODN and Stat3 dimer. We have used the SAR successfully in a well-established docking program for drug design and screening (Appendix 2). This system enables prediction of drug properties, such as efficiency, toxicity, and side effects, and can make backup available immediately when a candidate is found to have inadequate drug properties in clinical trials.

(2). A GQ-ODN T40214 was developed as a lead compound and determined to be a potent, specific inhibitor of Stat3 activation in several human cancer cells, such as breast (MDA-MB-468), hepatoma (HepG2), prostate (PC-3), and head and neck (167, B4B8) cancer cells, holding promise for the systemic treatment of many forms of human cancer.

(3) The stable G-quartet motifs are the primary determinants of the remarkable nuclease resistance and long-term biological efficacy of these oligonucleotides. The intramolecular G-quartet structure prevents single-strand endonucleases from accessing their cleavage sites, leading to a long oligonucleotide half-life inside cells (1). Also, the size of the G-quartet structure makes it possible to block target molecules with large active sites such as the SH2 domains of Stat3 homodimers.

(4). We have developed a novel and effective intracellular delivery system for G-quartet oligonucleotides (Appendix 1). The effective delivery of the GQ-ODNs into cancer cells is a key issue for success in cancer therapies that target oncogenic signaling intermediates. This delivery system greatly increased the delivery efficiency and drug activity of GQ-ODNs within cells. In addition to efficiently delivering GQ-ODNs into breast cancer cells in culture, this system was shown to be capable of delivering G-quartet inhibitors into animal tissues (Appendix 2).

(5). GQ-ODNs are low toxicity agents. Toxicity studies have been reported for a G-rich ODN, T30177 (or AR177), as an inhibitor of HIN-1 integrase (2). T30177 did not exhibit genetic toxicity in three different mutagenic assays: *Ames*/Salmonella mutagenesis assay, CHO/HGPRT mammalian cell mutagenesis assay, and mouse micronucleus assay. Acute toxicity studies in mice showed that T30177 has an LD50 (the lethal dose 50%) > or = 1.5g/kg body weight. Multiple dose toxicity studies in mice showed that T30177 did not cause male-specific mortality and changes in serum chemistry, hematology, and histology until doses reached 250 and 600 mg/kg, which are > 100 fold than the therapeutic level. The GQ-ODN T30177 forms the same intramolecular G-quartet structure with T40214 and T30923 (3, 4).

(6). Our *in vivo* data demonstrated that T40214 suppressed the growth of breast tumors *in vivo* by inhibiting Stat3 activation, resulting in the enhancement in the apoptosis of tumor cells. The mean

size of breast tumors in placebo-treated mice increased 7-fold while that of drug-treated mice remained unchanged (p=0.006) after treatment. Based upon the examinations of mean levels of phosphorylated Stat3 (p-Stat3), Bcl-x_L Bcl-2 and caspase 3 in the tumors of the drug-treated mice compared to the tumors from placebo-treated mice and TUNEL assays, we found that GQ-ODNs significantly increase apoptosis of tumor cells leading to suppress tumor growth.

To our knowledge, this is first demonstration that an agent that directly inhibits Stat3 activity is capable of suppressing tumor growth *in vivo*. Previous *in vivo* studies have employed JAK inhibitors, such as AG490 (5) and JSI-124 (6), which may target pathways downstream of JAK in addition to Stat3. Therefore, G-quartet ODN represents a novel, powerful, and potentially promising agent for treatment of breast cancer therapy.

IV. Conclusion.

Currently, chemotherapy is not very successful in prostate cancer and metastatic prostate cancer remains incurable using the currently available hormonal and chemotherapeutic treatments. Stat3 as a mediator of oncogenic signaling becomes a critical target for prostate cancer therapy since it is active in 82% of prostate cancers. The results in Appendix 1 and 2 demonstrated that GQ-ODN T40214 has dramatic *in vivo* effects on prostate cancer growth in nude mice when the agent is given by intravenous injection, dramatically retarding tumor growth and showing an obvious therapeutic effect. Also GQ-ODN T40214 greatly increases the number of apoptotic cells in tumors, indicating that the ODN is a potent agent using apoptosis to eliminate tumor cells in cancer therapy. Thus, GQ-ODNs represent a novel class of chemotherapeutic agents that holds promise for the systemic treatment of prostate cancer and also could be a powerful agent for other human cancers where Stat3 is active. This idea development award is very important for us to develop a novel anti-cancer drug for prostate cancer therapy. In this study, we also found that GQ-ONDs has strong therapeutic activity for breast cancer. Thus, we are planning to apply more funding form DOD for breast cancer therapy.

V. Reference.

1. Bishop J. B., Guy-Caffey, J. K. et al. G-quartet motifs confer nuclease resistance to a potent anti-HIV oligonucleotide. *J. Biol. Chem.* 271, 5698-5703 (1996).
2. Wallace, T. L., Gamba-Vitalo, C, Loveday, K. S., and Cossum, P. A. Acute, multipe-dose, and genetic toxicology of AR177, an anti-HIV oligonucleotide. *Toxicol. Sci.* 53, 63-70 (2000).
3. Jing, N., Gao, X. L., Rando, F. R., Hogan, M. E. (1997) Potassium-induced loop conformation transition of a potent anti-HIV ologonucleotide. *J. Biomol. Struct. & Dyn.* 15, 573-585.
4. Jing, N., Hogan, M. E. (1998) Structur-activity of tetrad-forming oligonucleotides as a potent anti-HIV therapeutic drug. *J. Biol. Chem.* 273, 34992-34999.
5. Burdelya, L., Catlett-Falcone, R., Levitzki, A., Cheng, F., Mora, L. B., Sotomayor, E., Coppola, D., Sun, J. Z., Sebti, S., Dalton, W. S., Jove, R., and Yu, H. Combination therapy with AG-490 and interleukin 12 achieves greater antitumor effects than either agent alone. *Mol. Cancer Therapeutics* 1, 893-899 (2002).
6. Blaskovich, M. A., Sun, J., Cantor, A., Turkson, J., Jove, R., and Sebti, S. M. Discovery of JSI-124 (Cucurbitacin I), a selective janus kinase/signal transducer and activitor of transcription 3 signaling pathway inhibitor with potent antitumor activity against human and murine cancer cells in mice. *Cancer Res.* 63, 1270-1279 (2003).

DNA AND CELL BIOLOGY
Volume 22, Number 11, 2003

Pp. 685–696

Targeting Stat3 with G-Quartet Oligodeoxynucleotides in Human Cancer Cells

NAIJIE JING,[1] YIDONG LI,[1] XUEJUN XU,[1] WEI SHA,[1] PING LI,[2]
LILI FENG,[2] and DAVID J. TWEARDY[1]

ABSTRACT

Stat3 is an oncogene that is activated in many human cancer cells. Genetic approaches that disrupt Stat3 activity result in inhibition of cancer cell growth and enhanced cell apoptosis supporting the development of novel drugs targeting Stat3 for cancer therapy. G-quartet oligodeoxynucleotides (ODNs) were demonstrated to be potent inhibitors of Stat3 DNA binding activity *in vitro* with the G-quartet ODN, T40214, having an IC_{50} of 7 μM. Computer-simulated docking studies indicated that G-quartet ODNs mainly interacted with the SH2 domain of Stat3 and were capable of inserting between the SH2 domains of Stat3 dimers bound to DNA. We demonstrated that the G-rich ODN T40214, which forms a G-quartet structure at intracellular but not extracellular K+ ion concentrations, is delivered efficiently into the cytoplasm and nucleus of cancer cells where it inhibited IL-6–stimulated Stat3 activation and suppressed Stat3-mediated upregulation of *bcl-x* and *mcl-1* gene expression. Thus, G-quartet represents a new class of drug for targeting of Stat3 within cancer cells.

INTRODUCTION

SIGNAL TRANSDUCER AND ACTIVATOR of transcription (STAT) 3 was originally termed acute-phase response factor (APRF) because it was first identified as a DNA-binding activity within IL-6–stimulated hepatocytes that was capable of selectively interacting with an enhancer element within the promoters of acute-phase response genes (Lutticken *et al.*, 1994; Raz *et al.*, 1994; Wegenka *et al.*, 1994; Zhong *et al.*, 1994). APRF or Stat3 was first purified to homogeneity and sequenced from the livers of IL-6–treated mice (Akira *et al.*, 1994). Receptors linked to Stat3 activation include receptors for the IL-6 cytokine family, granulocyte colony-stimulating factor (G-CSF), other type I and type II cytokine receptors, as well as tyrosine kinase-containing receptors and G-protein–coupled receptors (Schindler and Darnell, 1995). Stat3 activation downstream of these receptors has been demonstrated to influence multiple cell fate decisions including proliferation, apoptosis, and differentiation (Bromberg and Darnell, 2000).

In addition to serving as a signaling intermediate, Stat3 has been identified as a critical mediator of oncogenic signaling (Bromberg *et al.*, 1999; Bromberg and Darnell, 2000). Activation of Stat3 has been detected in many types of human cancers, and evidence has accumulated that Stat3 signaling is essential for their development and/or progression (Bowman *et al.*, 2000; Bromberg, 2001; Buettner *et al.*, 2002; Mora *et al.*, 2002). Stat3, like other members of the STAT protein family (1, 2, 4, 5A, 5B, and 6), is composed of several discrete domains including a tetramerization domain, a coiled-coil domain, a DNA-binding domain, a linker domain, a Src-homology 2 (SH2) domain, a tyrosine residue at position 705 that participates in dimerization, and a C-terminal transactivation domain (Zhang *et al.*, 1995). Stat3 exists in a latent form within the cytoplasm of ligand-unstimulated cells (Schindler and Darnell, 1995). Following binding of cytokines or growth factors to cognate receptors on the cell surface, Stat3 is recruited to receptor complexes where is becomes activated by phosphorylation on tyrosine 705. Tyrosine phosphorylation promotes dimer formation through reciprocal interaction between the SH2 domain of one Stat3 molecule and the phosphorylated C-terminal tyrosine 705 of its partner. The activated dimers translocate to the nucleus, where they bind to the promoters of target genes and activate gene transcription. The crystal structures of Stat3 and Stat1 homodimers demonstrated that the re-ciprocal interactions of the C-terminal phosphotyrosine and the SH2 domain hold the dimer together allowing the formation of a symmetric DNA

[1]Section of Infectious Diseases and [2]Section of Nephrology, Department of Medicine, Baylor College of Medicine, Houston, Texas.

duplex binding site (Becker *et al.*, 1998; Chen *et al.*, 1998). These structural features can be exploited to develop potent agents that inhibit Stat3 dimerization and DNA binding for potential use as cancer therapy.

G-rich oligodeoxynucleotides (ODN) have been identified, cloned, and characterized within the telemetric sequences of many organisms, such as fungi, ciliates, vertebrates, and insects (Henderson, 1995). Numerous investigations have shown that telemetric G-rich DNA and RNA can form intra- and intermolecular four-stranded structures, referred to as G-quartets (Williamson, 1994; Gilber and Feigon, 1999). G-quartets arise from the association of four G-bases into a cyclic Hoogsteen H-bonding arrangement with each G-base making two H-bonds with its neighbor G-base (N1 to O6 and N2 to N7). G-quartets stack on top of each other to give rise to tetrad-helical structures. Based upon the results of action-induced thermal stability of the G-quartet structure, selectivity of G-quartet formation in the presence of monovalent cations was proposed to be $K^+ > Rb^+ > Na^+ > Li^+$, or Cs^+ (Sen and Gilbert, 1990; Jing *et al.*, 1997), with K^+ having the optimal size to interact with and stabilize two sets of stacked G-quartets. Recently, G-quartet ODNs were designed that competed with HIV-1 DNA duplex to occupy the DNA-binding sites in the catalytic domain of HIV-1 integrase, thereby blocking integration of the virus into the host chromosome (Rando *et al.*, 1995; Mazumder *et al.*, 1996; Jing *et al.*, 2000a).

Based upon their ability to inhibit DNA binding proteins, we tested the G-quartet ODNs for the ability to inhibit Stat3. In the present report, we identified the G-quartet ODN T40214 as a new class of Stat3 inhibitor that was delivered efficiently into cells where it markedly inhibited IL-6–stimulated Stat3 activation and Stat3-mediated gene upregulation within human cancer cells.

MATERIALS AND METHODS

Oligodeoxynucleotides and cells

HLPC-purified ODN (Fig. 1A) were obtained from the Midland Certified Reagent Company, Inc. (Midland, TX) and used without further chemical modifications. The human hepatocarcinoma cell line, HepG2, was obtained from the ATCC and was grown in DMEM medium containing 10% fetal bovine serum with penicillin and streptomycin. Polyethylenimine (PEI, ~25 K, Aldrich Chemical, Milwaukee, WI) was generously provided by Dr. Charles Densmore (Baylor College of Medicine). Interleukin 6 (IL-6) and Interferon-γ (INF-γ were purchased from Santa Cruz Biotech Inc. (Santa Cruz, CA). Antibodies to Stat1 and Stat3 were purchased from Santa Cruz Biotech.

Circular dichroism (CD)

CD spectra of ODNs were performed at an ODN concentration of 15 μM in 10 mM KCl and 20 mM Li_3PO_4 at pH 7 and 24°C using a JASCO J-500A spectropolarimeter. Spectral data are presented in molar ellipticity ($deg \cdot cm^2 \cdot dmol^{-1}$), and represent the average of five scans.

Electrophoretic mobility shift assay (EMSA)

EMSA was performed as described (Tweardy *et al.*, 1995). Briefly, IL-6 (25 ng/mL) or INFγ (10 ng/mL) was added into the wells containing 5–7 $\times$ 10^5 HepG2 cells. Cells were washed and extracted using high-salt buffer. The protein concentrations of the extracts were determined using a Bradford assay (Sigma, St. Louis, MO). The ^{32}P-labeled duplex DNA probe (hSIE, 5′-AGCTTCATTTCCCGTAAATCCTA) was purified using G-25 columns (Amersham Pharmacia Biotech Inc., Arlington Hts, IL). A labeled hSIE probe was mixed with 5 μg of cell protein in 1 $\times$ binding buffer and 2 μg of poly-dIdC and incubated at room temperature (RT) for 15 min with or without G-quartet ODN. Samples were loaded onto 5% polyacrylamide gel containing 0.25 $\times$ TBE and 2.5% glycerol. The gel was run at 160–200 V for 2–3 h at room temperature, dried, and autoradiographed.

Treatment of cells with PEI G-quartet ODN:

G-quartet ODN with PEI at a weight ratio of PEI/ODN of 2:1 was added to cells (5–7 $\times$ 10^5). After incubation for 3 h, the cells were washed three times with fresh medium without PEI/ODN and the incubation continued. After 24 h, cells were incubated without or with IL-6 (25 ng/mL) at 37°C for 20 min before extraction and analysis by EMSA as described above.

Statistical docking calculations

The original molecular structures of Stat3β and Stat1 were obtained from the Protein Data Bank (Becker *et al.*, 1998; Chen *et al.*, 1998). The coordinated files of the structures of two STAT monomers were modified into a structure of STAT homodimers with a 20 base-pair DNA duplex (hSIE) on a SGI computer workstation. The NMR structure of T30923 (originally named T30695) (Jing and Hogan, 1998) was docked onto our model of Stat3β and Stat1 homodimers using the GRAMM docking program in the high-resolution matching mode (Katchalski-Katzri *et al.*, 1992; Vakser, 1996). This program uses a geometry-based algorithm for predicting the structure of a possible complex between molecules of known structures. It can provide quantitative data related to the quality of the contact between the molecules. The intermolecular energy was calculated from well-established correlation and Fourier transformation techniques used in field-of-pattern recognition. The docking calculation by GRAMM constructed the complexes composed of the STAT dimers and the G-quartet ODN using their atomic coordination, without any prior information as to their binding sites. The distributions of the H-bond formation between the amino acid residues of Stat3 or Stat1 dimer and T30923 were calculated and analyzed for each complex.

Intracellular delivery of radiolabeled G-quartet ODN

The details of the methods were described previously (Jing *et al.*, 2002). Briefly, ODNs in H_2O were heated at 90°C for 15 min and then cooled down to RT. ODNs were labeled with ^{32}P by 5′-end labeling and purified using G-25 spin columns. The ^{32}P-labeled ODNs were incorporated with PEI at a weight ratio of PEI/ODN of 2:1 at RT for 1 h. Labeled ODNs (700 ng) were added to wells containing 5 $\times$ 10^5 cells. After 3 h incubation in PEI/ODN, the cells were washed three times with fresh medium without PEI/ODN then incubated at 37°C for 24 h. Cells were washed three times with PBS, and transferred to a culture tube and lysed with lysis buffer. Lysates were spun to

A. DNA oligonucleotides
(1) T30923: GGGTGGGTGGGTGGGT
(2) T40214: GGGCGGGCGGGCGGGC
(3) T40216: GGGGGTGGGGGTGGGGTGGGGGT
(4) nonspecific ODN: TGCCGGATCAAGAGCTACCA

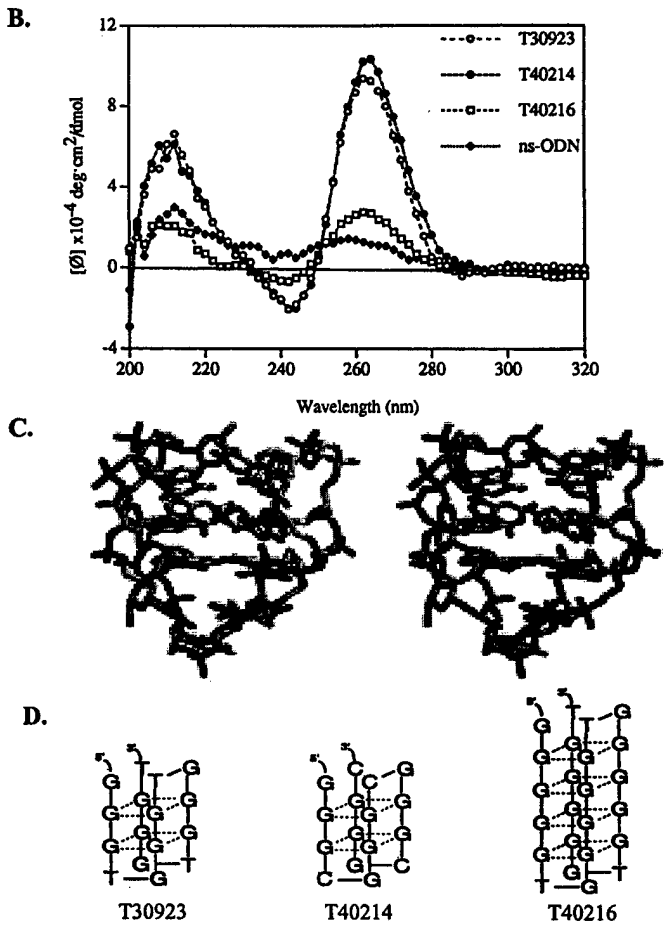

FIG. 1. Sequences and structures of G-rich ODNs. The nucleotide sequences of the G-rich ODNs, T30923, T40214, T40216, and the nonspecific (ns) ODN synthesized are shown in (**A**). (**B**) The CD spectra of T30923, T40214, T40216, and ns-ODN are shown, indicating that T40214 and T40216 formed a G-quartet structure similar to T30923 while the ns-ODN did not. In (**C**), stereoviews of the NMR structure of T30923 are shown, which reveal two G-quartets in the center and two loop domains, one at the top and one at the bottom. (**D**) Shows a model of each of the G-quartet-forming ODNs, T30923, T40214, and T40216. G-bases forming a cyclic Hoogsteen H-bonding arrangement are connected by dashed lines.

remove cell debris. ODN within the supernatants were precipitated by addition of ethanol, pelleted, dried, resuspended, and loaded onto 20% nondenaturing polyacrylamide gels run at 4°C.

Microscopy

Cells were incubated with fluorescein-labeled oligonucleotide T40214 complexed with PEI at a weight ratio of PEI/DNA of 2:1. After incubation for 3 h, the cells were washed three times with fresh medium without PEI/ODN and the incubation continued at 37°C for 24 h. Cells were washed three times with PBS, stained with DAPI, incubated with 0.5% Triton X-100 for 2 min then fixed on slides for 15 min in 3.7% formaldehyde. Slides were washed three times with PBS and examined by fluorescence microscopy at 400× magnification.

RNase protection assay (RPA)

RPA was performed using an RPA kit as outlined by the manufacturer (Torrey Pines Biolabs, Inc., Houston, TX). Briefly, pooled DNA templates were added into reaction mixtures containing RNA polymerase, ^{32}P-UTP and DNase and incubated at 37°C for 30 min. The reactions were stopped by addition of 15μl of 20 mM EDTA. The resulting antisense

RNA probes were purified through a G-50 spin column and 0.5–1.0 × 10^5 cpm added to the sample RNA. The mixture was incubated at 90°C for 25 min and allowed to cool to RT. RNase was added to each tube and incubated at RT for 30 min. Undigested RNA was precipitated, washed, dissolved in 5 μl of loading buffer, heated at 90°C for 3 min, and immediately transferred to wet ice then loaded onto a 6% sequencing gel run at 400–450 V.

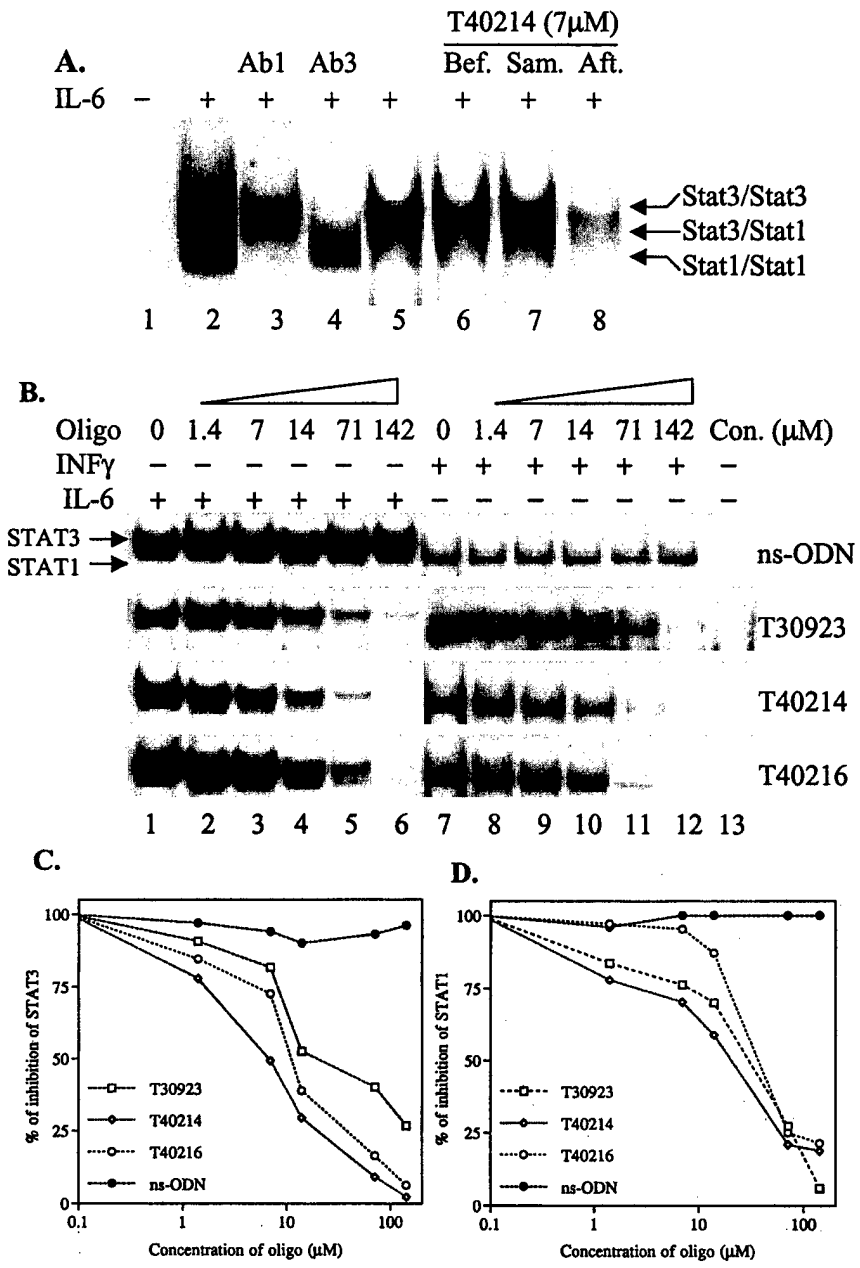

FIG. 2. Inhibition of IL-6–stimulated Stat3 activation by G-quartet ODN. (**A**) EMSA was performed using extracts of HepG2 cells incubated without (−) or with (+) IL-6. The composition of the bands corresponding to Stat1 and Stat3 dimers were confirmed using blocking antibodies against Stat1 (lane 3) and Stat3 (lane 4), respectively. Binding reactions are performed without (−) or with (+) T40214 (7 μM) added at different times relative to addition of hSIE duplex oligonucleotide (lane 5, without adding T40214; lane 6, adding T40214 before addition of hSIE; lane 7 adding T40214 at the same time as addition of hSIE; lane 8, adding T40214 after the addition of hSIE). (**B**) Autoradiagraphs of EMSA gels demonstrating the effects of addition of increasing amounts of ODNs on DNA-binding activity of Stat3 (lanes 2–6) and of Stat1 (lanes 8–12). Lane 13 is a negative control. Densitometric analyses of the intensities of the bands of Stat3 and Stat1 homodimer are shown in (**C**) and (**D**), respectively.

TABLE 1. INHIBITORY CONCENTRATION (IC_{50}) OF ODNS FOR STAT3 AND STAT1

ODN	*IC_{50} to Stat3 (μM)*	*IC_{50} to Stat1 (μM)*
T30923	25	41
T40214	7	27
T40216	12	48
ns-ODN	—	—

RESULTS

Structure of G-quartet ODNs

We employed three G-rich ODNs capable of forming G-quartets and one nonspecific ODN to examine Stat3 targeting in cancer cells (Fig. 1A). The molecular structure of the G-rich ODN, T30923 (also called T30695), with the sequence $(GGGT)_4$ has been determined by NMR to have an intramolecular G-quartet structure, composed of two G-quartets in the center and two T-G-T-G loop domains on the top and bottom (Fig. 1C) (Jing and Hogan, 1998). This G-quartet structure is very compact, with a 15 Å width and a 15 Å length. The distance between the two central G-quartet planes is about 3.9 Å. The G-rich ODNs, T40214 and T40216, with the sequences of $(GGGC)_4$ and $(GGGGGT)_4$, respectively, also have been demonstrated to form intermolecular G-quartet structures (Fig. 1D) (Jing *et al.*, 2000b, 2002). The G-quartet forming ODNs were characterized by CD (circular dichroism) spectra with a maximum at 264 nm and a minimum at 240 nm (Fig. 1B). CD spectra showed that T40214 and T40216 ODNs formed the same molecular structure as that of T30923. T40216 has a

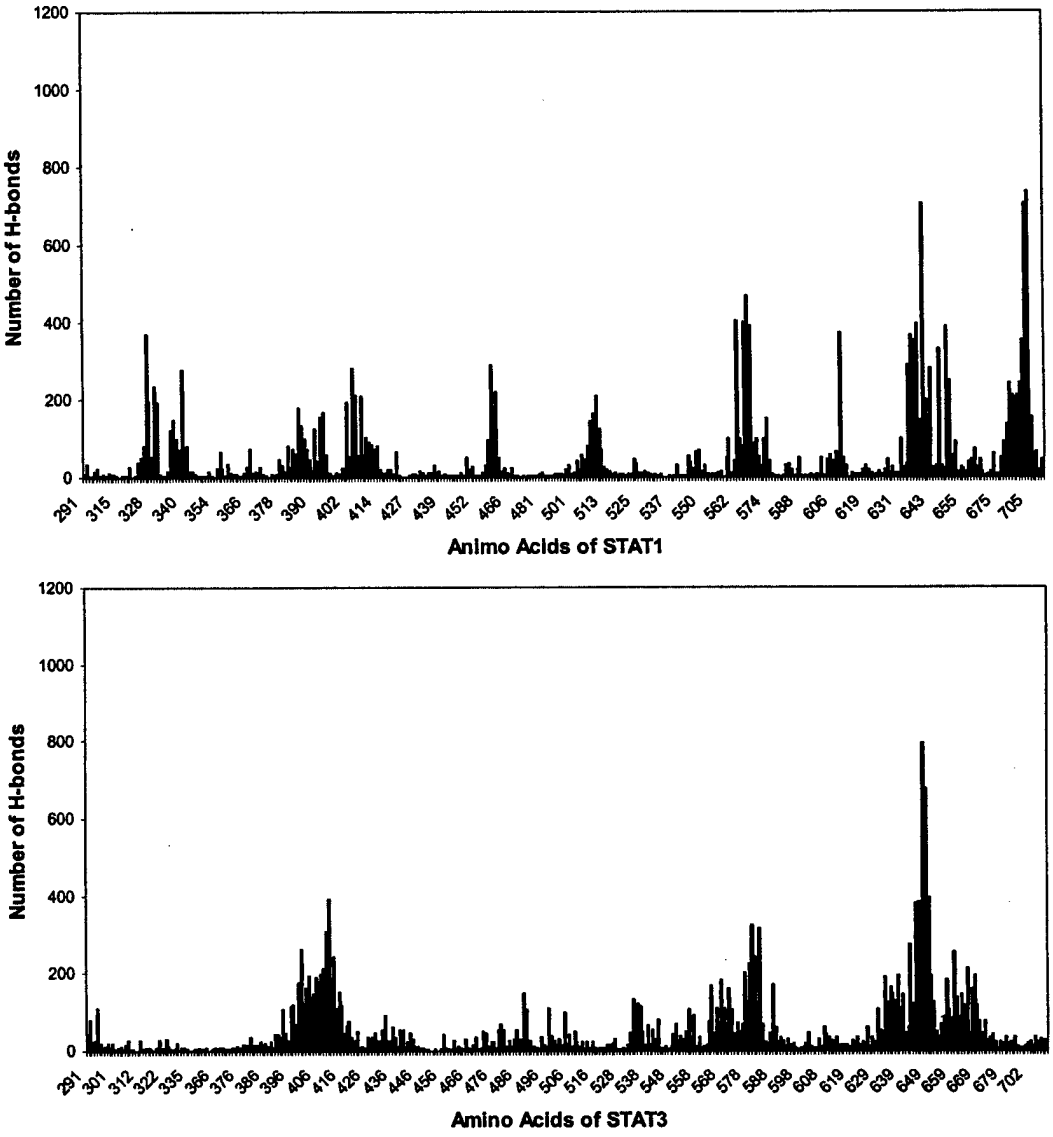

FIG. 3. Histograms of the distributions of H-bonds formed between G-quartet ODN T30923 and Stat1 (upper panel) and between G-quartet ODN and Stat3 (lower panel) based upon computer analyses of two thousand docking interactions (see text for details).

longer G-quartet stem of about 24 Å in length containing four G-quartets. The weaker CD ellipticity at 264 and 240 nm indicated that the stability of G-quartet structure of T40216 was much less than that of T30923. T40214 differs from T30923 by substitution of cytosines for thymines in the loop domains. These substitutions decreased the binding affinity to K^+ ions such that T40214 forms a G-quartet at intracellular but not extracellular K^+ concentrations resulting in increased efficiency of intracellular delivery (Jing *et al.*, 2002). The CD spectra of ns-ODN did not show ellipticities at 264 and 240 nm, characteristic of a G-quartet structure, indicating that the nonspecific ODN does not form a G-quartet structure.

Inhibition of Stat3 DNA binding by G-quartet ODN

Inhibition of Stat3 DNA-binding activity by G-quartet ODN was assessed by electrophoretic mobility shift assay (EMSA). Extracts of IL-6–stimulated HepG2 cells formed three bands comprised of Stat3 homodimers, Stat1 homodimers and Stat1/Stat3 heterodimers (Fig. 2A). The composition of the STAT dimers was confirmed using blocking antibodies to Stat1 (lane 3) and Stat3 (lane 4). To determine whether G-quartet ODNs interfered with Stat3 or Stat1 DNA binding, we added G-quartet ODN, T40214 (7 μM), to binding reactions before, concurrent with or after addition of the hSIE probe. No inhibition of DNA-binding activity was observed when T40214 was added before or at the same time as the hSIE probe (lanes 6 and 7). However, strong inhibition of DNA-binding activity was observed when T40214 was added 15 min after addition of the hSIE probe (lane 8) with inhibition of Stat3 predominating. These results indicated that G-quartet ODNs were capable of destabilizing Stat3 dimers following their binding to hSIE.

To confirm that the effect of G-quartet ODNs was more specific for Stat3 versus Stat1, we examined the effect of G-quartet ODN on the DNA binding activity of Stat3 and Stat1 within extracts of IL-6– and IFNγ-stimulated HepG2 cells, respectively (Fig. 2B–D). The 50% inhibitory concentration (IC_{50}) of T30923, T40214, and T40216 for Stat3 were 25, 7, and 12 μM, respectively (Table 1). In each case, the respective IC_{50} for Stat1 was two- to fourfold higher than that for Stat3, indicating preferential inhibition of Stat3. Of the three G-quartets studied, T40214 was the most active inhibitor of Stat3 DNA binding. The IC_{50} of T40214 for Stat3 (7 μM) was almost four times lower than its IC_{50} for Stat1 (27 μM). In contrast to the G-quartet ODNs, the ns-ODN did not inhibit the DNA binding of either Stat3 or Stat1 homodimers, indicating that the intramolecular G-quartet structure was required to inhibit the DNA binding of STAT dimers.

Computer-based examination of G-quartet ODN interactions with Stat3 and Stat1

To determine the mechanism of inhibition by G-quartet ODN of STAT DNA-binding activity and to gain insight into their preferential inhibition of Stat3, we employed computer-base statistical docking calculations to estimate the probability of interaction between drug and target molecules and to identify the potential binding sites on the target molecule. We docked the NMR structure of T30923 (Jing and Hogan, 1998) onto the crystal structure of Stat3β and Stat1 homodimer (Becker *et al.*, 1998; Chen *et al.*, 1998) using the GRAMM docking program without setting any binding site restrictions. The docking range for T30923 with the Stat3 and Stat1 dimers was established from amino residues 291 to 716 of one STAT protein and included amino residues 716 to 291 of the other STAT protein. These residues included several critical STAT protein domains: the coiled-coil domain, the DNA-binding domain, the linker domain, the SH2 domain, and the C-terminal domain containing the phosphorylated tyrosine 705 (Stat3) or 701 (Stat1). The number of H-bonds was calculated for each binding interaction. Two thousand possible interactions were analyzed and revealed that the total number of H-bonds formed between T30923 and Stat3 dimer was 20,948 and between T30923 and Stat1 was 20,864. Histogram analysis of H-bond distributions demonstrated that G-quartets predominantly interacted with three or four regions within the four domains of the STAT protein (Fig. 3 and Table 2). Region 1 consisted of residues 396 to 416 within the critical domain for DNA binding. Regions 2 and 3, which consist of residues of 577 to 591 and 633 to 670, are contained within the SH2 domain critical for STAT dimerization. Region 4 consisted of residues 680 to 706 in the region, which contains the phosphorylated tyrosine important for dimer formation. Further examination of the H-bond histograms (Fig. 3) revealed that the interactions between the G-quartet ODN and Stat3 are concentrated in Regions 1, 2, and 3, while the interactions between G-quartet ODN and Stat1 were more widely distributed over the Stat1 structure. Sixty-one percent of G-quartet ODN–Stat3 interaction occurred within Regions 1 to 4 of Stat3 compared with only 44% of G-quartet ODN–Stat1 interactions. Furthermore, 43% of G-quartet H-bonds formed with Stat3 occurred with regions contained within the SH2 and phosphorylated tyrosine domains required for dimerization compared to 38% of bonds formed with Stat1. Docking analysis using a modeled structure of T40214 obtained by modifying the NMR structure of T30923 using the INSIGHTII program demonstrated H-bond histograms for Stat3 and Stat1 virtually identical to that obtained for T30923 (data not shown).

A model of G-quartet ODN targeting of Stat3 dimer was obtained from the GRAMM docking analysis (Fig. 4). In this

TABLE 2. DISTRIBUTION OF H-BONDS FORMED BETWEEN G-QUARTETS AND STAT PROTEINS

Region	*Amino acids of STAT proteins*	*Domains of STAT proteins*	*% of total H-bonds formed with Stat3*	*% of total H-bonds formed with Stat1*
1	396–416	DNA binding	18	6
2	577–591	SH2	10	0.7
3	633–670	SH2	31	25
4	680–716	C-terminal	2	12
1–4	—	—	61	43.7

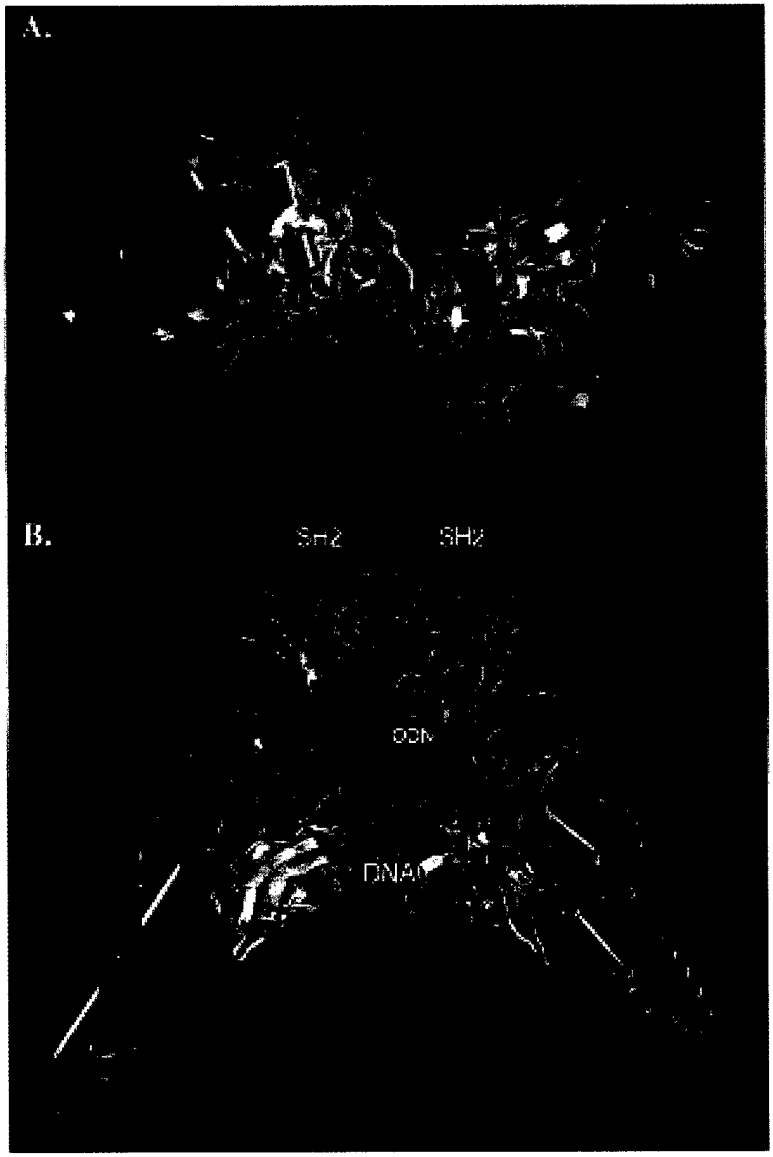

FIG. 4. Top view (**A**) and side view (**B**) of the binding complex of the G-quartet ODN and Stat3 dimer. The ODN (T30923) is shown in green. Different domains of Stat3 are depicted: blue for loops, red for α-helixes, and yellow for β-sheets. The hSIE duplex is shown in brown. T30923 is shown inserting into the SH2 domains of Stat3 dimer and symmetrically formed H-bonds with amino residues from 642 to 450 within each monomer of Stat3. The loop residues at each end of T30923 showed strong interaction with the Stat3 dimer. G1, G2, T4, and G5 of one surface interacted with one monomer while G9, G10, T12, and G13 of the opposite surface of the ODN interacted with the SH2 domain of the other monomer.

model, T30923 inserts between the two SH2 domains of the Stat3β dimer. A binding site between the G-quartet ODN and Stat3 dimer was determined based upon statistical calculations, in which H-bonds are formed between one surface of T30923 and residues 643 to 648 in one monomer of Stat3 and the opposite surface of T30923 and identical residues within the other Stat3 monomer. The H-bonds formed occur between G1 N_9H and Q643 $O_\epsilon 1$; G2 N_3H and Q643 CO; G2 O4′ and Q644 $O_\epsilon H$; G2 N_2H and N646 C_δ; G5 N_2H and N646 CO; G2 O3′ and N647 $N_\delta H$; T4 O3′ and C648 NH; G5 PO_2 and C648 NH in one monomer. This model suggests that G-quartet ODNs interact with residues from 643 to 648 and destabilize Stat3 dimers because these residues played key roles in Stat3-phosphotyrosine interactions essential for dimerization (Becker *et al.*, 1998). Of note, the loop domains of G-quartet ODNs, including G1 (or G2)-T8-G9-T16 and T4-G5-T12-G13, were found to play important roles in the interaction between G-quartet ODN and Stat3.

Intracellular and intranuclear delivery of G-quartet ODNs

A system of delivering G-quartet ODNs into cells and nuclei (Fig. 5A) has recently been developed (Jing *et al.*, 2002). In the studies reported here, we used polyethylenimine (PEI) instead of lipid as a carrier. To demonstrate intracellular delivery of G-quartet ODN, ^{32}P-labeled ODNs, with PEI at a ratio of PEI:ODN of 2:1 were incubated with HepG2 cells for 3 h at 37°C. Twenty-four hours later, cells were extracted and ODN within cells analyzed on a nondenatured gel (Fig. 5B). The densitometric analysis of the ODN bands estimated that the percentage of ODN released from PEI/ODN complexes into cytoplasm at 24 h was 34% for T40214, 31% for T30923, 20% for ns-ODN, and 14% for T40216. T40216, with the longest sequence, had the lowest delivery efficiency. Judging from the band of free G-quartet ODN on the gel (lane 2), most of the G-rich ODNs, T40214, and T30923, released within cells formed G-quartet structures. In contrast, ns-ODN released within cells did not form a G-quartet structure (lane 1).

The size of G-quartets should allow them to passively diffuse from the cytoplasm into the nuclear through nucleus pores. Entry of G-quartet ODNs into the nucleus of HepG2 cells was confirmed using the fluorescent-labeled T40214 complexed with PEI (Fig. 5C).

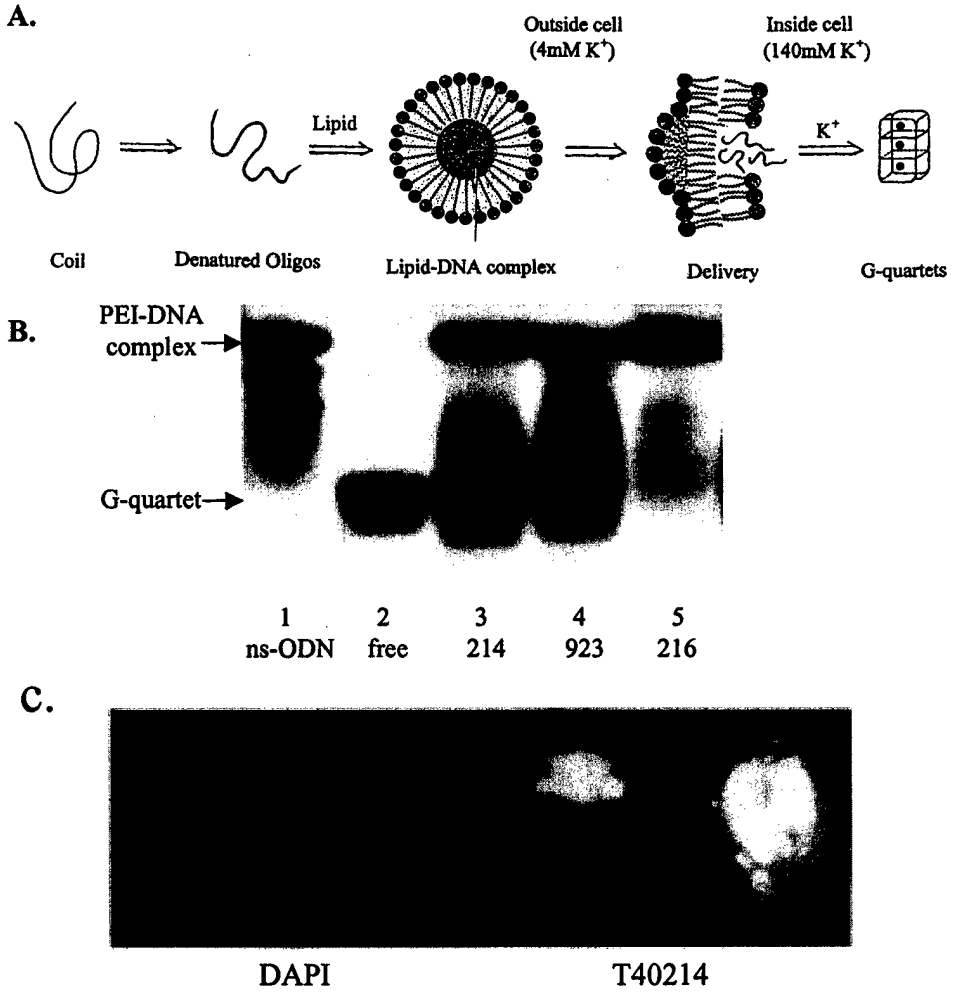

FIG. 5. Intracellular delivery of G-quartet ODN. (**A**) Depicts a schematic model of the delivery system. This system includes several steps: (i) G-rich ODN were denatured to increase complex formation between ODNs and carrier. (ii) The lipid–ODN complexes bind to the membranes of cells releasing ODN into the cytoplasm. (iii) The released ODN molecules form the G-quartet structure, induced by the high concentration of K^+ ions inside cells, and interact with the target proteins. (**B**) An autoradiograph of a nondenaturing gel demonstrating that the molecules of ODNs were delivered inside cells and formed G-quartets in the cytoplasm. Lane 2 is free T40214 in the G-quartet structure as a control. Lane 1, 3, 4, and 5 are ^{32}P-labeled ns-ODN, T40214, T30923, and T40216, respectively, extracted from cells following incubation of cell with the PEI/ODN complex at 2:1 for 3 h and harvested 24 h later. (**C**) Flourescent micrographs of cells visualized for DAPI staining (left panel) and fluorescein-labeled T40214 (right panel) demonstrating localization of T40214 within the nucleus.

Inhibition of Stat3 activation within cells by G-quartet ODN

To determine if G-quartet ODNs can inhibit Stat3 activation within human cancer cells, we incubated HepG2 cells with PEI/G-quartet ODN for 3 h then stimulated them with IL-6 24 h later. The level of inhibition of Stat3 activation in cells was greatest for T40214, achieving 90% at a concentration of 50 ng/μl and resulted in 60% inhibition at 1 ng/μl. In contrast, preincubation with ns-ODN had no effect on Stat3 DNA activation by IL-6 (Fig. 6B). The lower level of inhibition of Stat3 activation in cells by T40216 may be due to its lower efficiency of intracellular delivery.

Suppression of Stat3-induced gene upregulation

To determine if inhibition of Stat3 DNA binding activity within cells by G-quartet ODN resulted in suppression of Stat3-induced gene upregulation, we performed RNAse protection assays to examine mRNA levels of Stat3-regulated genes. Preincubation of HepG2 cells with increasing concentrations of T40214 demonstrated that upregulation of Bcl-x mRNA was completely inhibited, while upregulation of Mcl-1 mRNA was suppressed about 50% at 50 ng/μl (Fig. 7A and B). In contrast, preincubation of cells with T40214 had no effect on levels of GAPDH and L32 mRNA. The result indicated that delivery of G-quartet ODNs within cells specifically suppressed the expression of Stat3-regulated genes, including those such as *bcl-x* and *mcl-1* important for cancer cell survival.

DISCUSSION

Stat3 has emerged recently as a novel and potentially important target for cancer drug discovery (Turkson and Jove, 2000). Evidence is mounting from studies of tumor cell lines and tumor samples that Stat3 is a critical mediator of oncogenic signaling and participates in the development and/or progression of a number of human malignancies, including breast, prostate, ovarian, head and neck cancer (Bowman *et al.*, 2000; Bromberg and Darnell, 2000; Buettner *et al.*, 2002). We demonstrated that G-quartet ODNs destabilized STAT dimers following their binding to duplex DNA showing preferentially activity against DNA binding of Stat3 versus Stat1. Computer-based docking analysis revealed that G-quartet ODN interacted with Stat3 dimer predominantly in the regions involved in dimerization. The percentage of G-quartet interactions with these regions within Stat3 (43%) was higher than that for the corresponding regions of Stat1 (38%), which may account, in part, for their more effective destabilization of Stat3. The G-quartet ODN, T40214, which formed a G-quartet structure at intracellular but not extracellular K^+ concentration, was delivered efficiently into the cytoplasm and nuclei of cells and

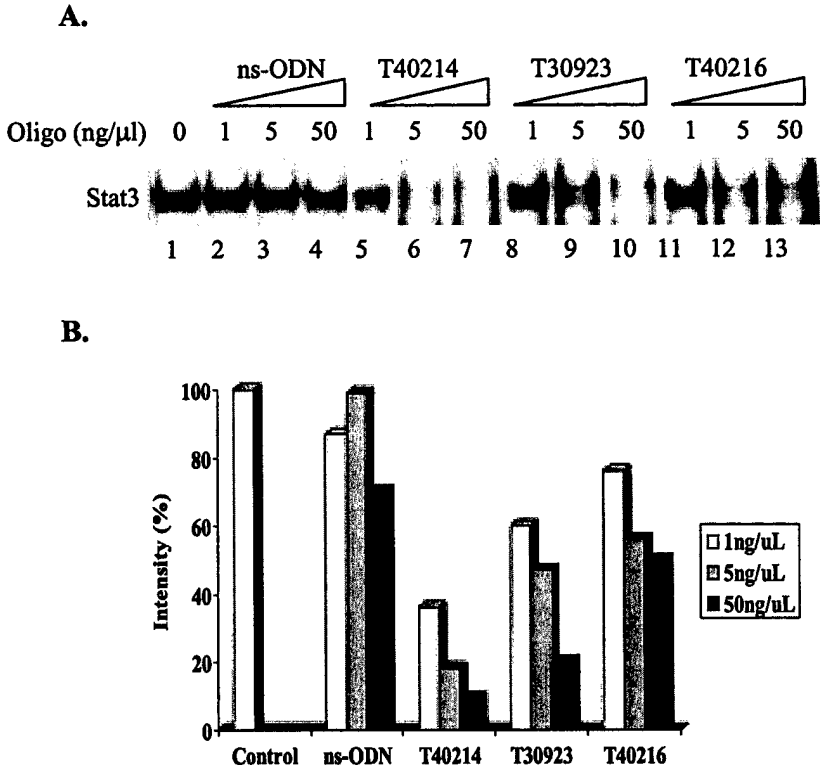

FIG. 6. Inhibition of Stat3 activation within cells and nuclei by G-quartet ODNs. Cells were stimulated with IL-6 24 h after incubation with PEI/ODN. (**A**) Autoradiograph of EMSA demonstrating inhibition of Stat3 activation in whole-cell extracts of HepG2 cells by G-quartet ODNs. (**B**) The plot demonstrates the concentration-dependent inhibition of Stat3 DNA-binding activity for the four ODNs in $HepG_2$ cells. The intensity of the bands were plotted as a percent of the band in the untreated line (control).

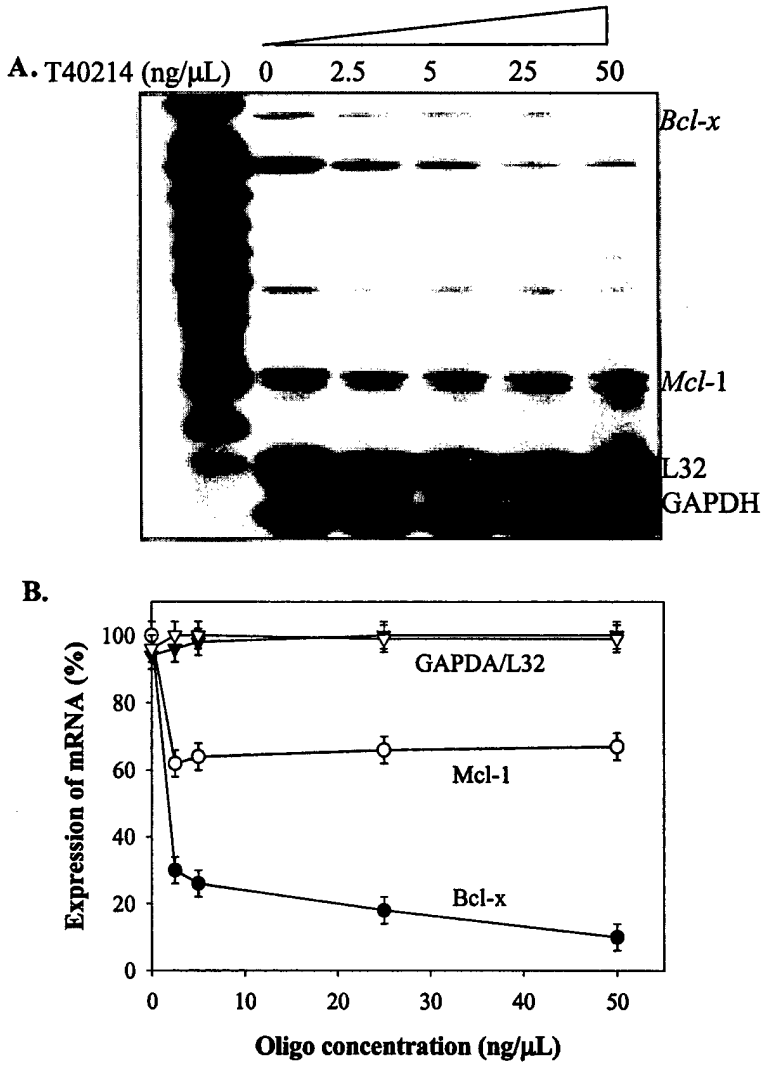

FIG. 7. Inhibition of Stat3 gene upregulation by G-quartet ODN. Total RNA was harvested from the plates containing cells incubated with T40214 24 h earlier then stimulated with IL-6 for 30 min. (**A**) Equal amounts of RNA were incubated with radiolabeled antisense RNA for bcl-x, Mcl-1, L32, and GAPDH followed by RNase treatment. Samples were separated by gel electrophoresis and the gel autoradiographed. (**B**) Densitometric analysis of the autoradiograph in (**A**) was performed, and the results presented as the mean ± SD of triplicate determinations.

was able to inhibit IL-6–stimulated Stat3 activation and upregulation of *bcl-x* and *mcl-1* gene expression. Thus, G-quartet ODNs represent a new class of drug for targeting Stat3 activated within cancer cells.

The *bcl-x* gene encodes two isoforms of Bcl-x: a long (L) and short (S) form. Bcl-x_L is an antiapoptotic protein within Bcl-2 family and the major protein isoform present within cells (Grad *et al.*, 2001). High levels of Bcl-x_L expression were associated with advanced disease and poor prognosis in several tumor systems (Boise *et al.*, 1993; Gonzalez-Garcia *et al.*, 1994). The *mcl-1* gene regulated by Stat3 also represents a survival factor for human cancer cells (Zhou *et al.*, 1997; Epling-Burnette *et al.*, 2001). Agents that reduce the levels of *bcl-x* and *mcl-1* gene expression may prove useful in cancer therapy by inducing cell apoptosis. Studies are underway to examine the effects of G-quartet ODN on the growth and apoptosis of cancer cells that demonstrate aberrant Stat3 activation.

Effective delivery of drug into cells is critical for development of a successful cancer therapy targeting Stat3. Recently, we have developed an effective intracellular delivery system for G-quartet ODNs that exploits the difference of K^+ concentration outside (4 mM) and inside (140 mM) cells (Jing *et al.*, 2002). In this report, we demonstrated that PEI serves as an effect alternative for lipid as a carrier. Once delivered into the cytoplasm of cells where the K^+ concentration is high, the G-rich ODN form G-quartet structures. In addition to permitting passive diffusion into the nucleus, the compact G-quartet size and structure prevents single-strand endonucleases from ac-

cessing their cleavage sites, leading to a long half-life within the cytoplasm and nucleus of cells (Bishop *et al.*, 1996).

Inhibition of DNA-binding activity of Stat3 by G-quartet ODN occurred when added to Stat3 homodimers after but not before addition of hSIE. These findings strongly suggest that inhibition occurs through binding of G-quartet ODN to the SH2 domains resulting in destabilization of the homodimer rather than by direct inhibition of DNA binding. Furthermore, these findings suggest that binding of Stat3 to hSIE duplex DNA induces a structural change within the SH2 domains of the Stat3 homodimer that allows greater access of the G-quartet to the SH2 domains.

In contrast to Stat3, Stat1 has been suggested to have a negative effect on cell growth (O'Shea *et al.*, 2002). Therefore, one of our goals is to design a G-quartet ODN that targets Stat3 while sparing Stat1. Achieving this goal will be a challenge, because the crystal structure of Stat3 homodimer bound to duplex DNA is very similar to that of Stat1 homodimer (Becker *et al.*, 1998; Chen *et al.*, 1998). Furthermore, Stat3 and Stat1 share more than 50% amino acid sequence homology in the region of the SH2 domain. Our results thus far, however, are encouraging in this regard demonstrating that the G-quartet ODN T40214 inhibited the DNA-binding activity of both Stat3 and Stat1 but showed fourfold greater activity against Stat3 versus Stat1. These findings indicate some selectivity in targeting Stat3, which our computer-based docking studies were able to attribute to preferential targeting of the dimerization domains of Stat3 versus Stat1. Studies are underway to design G-quartet ODNs with greater selectivity for Stat3 versus Stat1 using the computer-based modeling studies combined with DNA binding studies as outlined in this report.

ACKNOWLEDGMENTS

The authors would like to thank Dr. Charles Densmore for the gift of PEI stock solution and Weijun Xiong for obtaining Figure 5C. This work was supported by DOD Award PC020407 (N.J.) and NH Grants GM60153 (N.J.), CA 86430 (D.J.T.), and CA72261 (D.J.T.).

REFERENCES

AKIRA, S., NISHIO, Y., INOUE, M., WANG, X.J., WEI, S., MATSUSAKA, T., YOSHIDA, K., SUDO, T., NARUTO, M., and KISHIMOTO, T. (1994). Molecular cloning of APRF, a novel IFN-stimulated gene factor 3 p91-related transcription factor involved in the gp130-mediated signaling pathway. Cell **77,** 63–71.

BECKER, S., GRONER, B., and MULLER, C. (1998). Three-dimensional structure of the Stat3β homodimer bound to DNA. Nature **394,** 145–150.

BISHOP, J.S., GUY-CAFFEY, J.K., OJWANG, J.O., SMITH, S.R., HOGAN, M.E., COSSUM, P.A., RANDO, R.F., and CHAUDHARY, N. (1996). G-quartet motifs confer nuclease resistance to a potent anti-HIV oligonucleotide. J. Biol. Chem. **271,** 5698–5703.

BOISE, L.H., GONZALEZ-GARCIA, M., POSTEMA, C.E., DING, L., LINDSTEN, T., TURKA, L.A., MAO, X., NUNEZ, G., and THOMPSON, CB. (1993). Bcl-x, a bcl-2–related gene that functions as a dominant regulator of apoptotic cell death. Cell **74,** 597–608.

BOWMAN, T., GARCIA, R., TURKSON, J., and JOVE, R. (2000). STATs in oncogenesis. Oncogene **19,** 2474–2488.

BROMBERG, J.F., WRZESZCZYNSKA, M.H., DEVGAN, G., ZHAO, Y., PESTELL, R.G., ALBANESE, C., and DARNELL, J.E. (1999). Stat3 as an oncogene. Cell **98,** 295–303.

BROMBERG, J., and DARNELL, J.E. (2000). The role of STATs in transcriptional control and their impact on cellular function. Oncogene **19,** 2468–2473.

BROMBERG, J.F. (2001). Activation of STAT proteins and growth control. BioEssay **23,** 161–169.

BUETTNER, R., MORA, L.B., and JOVE, R. (2002). Activated STAT signaling in human tumor provides novel molecular targets for therapeutic intervention. Clin. Cancer Res. **8,** 945–954.

CHEN, X., VINKEMEIER, U., ZHAO, Y., JERUZALMI, D., DARNELL, J.E., and KURIYAN, J. (1998). Crystal structure of a tyrosine phosphorylated Stat-1 dimer bound to DNA. Cell **93,** 827–839.

EPLING-BURNETT, P.K., LIU, J.H., CATLETT-FALCONE, R., TURKSON, J., OSHIRO, M., KOTHAPALLI, R., LI, Y., WANG, J.M., YANG-YEN, H.F., KARRAS, J., *et al.* (2001). Inhibition of STAT3 signaling leads to apoptosis of leukemic large granular lymphocytes and decrease Mcl-1 expression. J. Clin. Invest. **107,** 351–362.

FUKADA, T., OHTANI, T., YOSHIDA, Y., SHIROGANE, T., NISHIDA, K., NAKAJIMA, K., HIBI, M., and HIRANO, T. (1998). Stat3 orchestrates contradictory signals in cytokine-induced G1 to S cell-cycle transition. EMBO J. **15,** 6670–6677.

GILBER, D.E., and FEIGON, J. (1999). Multistranded DNA structures. Curr. Opin. Struct. Biol. **9,** 305–314.

GONZALEZ-GARCIA, M., PEREZ-BALLESTERO, R., DING, L., DUAN, L., BOISE, L.H., THOMPSON, C.B., and NUNEZ, G. (1994). Bcl-x_L is the major bcl-x mRNA form expressed during murine development and its product localizes to mitochondria. Development **120,** 3033–3042.

GRAD, J.M., ZENG X.R., and BOISE, L.H. (2001). Regulation of Bcl-x_L: A little bit to this and a little bit to STAT. Curr. Opin. Oncol. **12,** 543–549.

GRANDIS, J.R., DRENNING, S.D., ZENG, Q., WATKINS, S.C., MELHEM, M.F., ENDO, S., JOHNSON, D.E., HUANG, L., HE, Y., and KIM, J.D. (2000). Constitutive activation of stat3 signaling abrogates apoptosis in squamous cell carcinogenesis in vivo. Proc. Natl. Acad. Sci. USA **97,** 4227–4232.

HENDERSON, E. (1995). *Telomeres* (Cold Spring Harbor Laboratory Press, Cold Spring Harbor, NY), pp 11–34.

JING, N., and HOGAN, M.E. (1998). Structure–activity of tetrad-forming oligonucleotides as a potent anti-HIV therapeutic drug. J. Biol. Chem. **273,** 34992–34999.

JING, N., MARCHAND, C., GUAN, Y., LIU, J., PALLANSCH, L., LACKMAN-SMITH, C., DE CLERCQ, E., and POMMIER, Y. (2000a). Stability–activity relationships of a family of G-tetrad forming oligonucleotides as potent HIV inhibitors. J. Biol. Chem. **275,** 3421–3430.

JING, N., MARCHAND, C., LIU, J., MITRA, R., HOGAN, M.E., and POMMIER, Y. (2000b). Mechanism of inhibition of HIV-1 integrase by G-tetrad forming oligonucleotides. J. Biol. Chem. **275,** 21460–21467.

JING, N., RANDO, F.R., POMMIER, Y., and HOGAN, M.E. (1997). Ion selective folding of loop domains in a potent anti-HIV oligonucleotide. Biochemistry **36,** 12498–12505.

JING, N., XIONG, W., GUAN, Y, PALLANSCH, L., and WANG, S. (2002). Potassium dependent folding: A key to intracellular delivery of G-quartet oligonucleotides as HIV inhibitors. Biochemistry **41,** 5397–5403.

KATCHALSKI-KATZRI, E., *et al.* (1992). Molecular surface recognition: Determination of geometric fit between proteins and their ligands by correlation techniques. Proc. Natl. Acad. Sci. USA **89,** 2195–2199.

LIN, J., JIN, X., ROTHMAN, K., LIN, H.-J., TANG, H., and BURKE, W. (2002) Modulation of signal transducer and activator of transcription 3 activities by p53 tumor suppressor in breast cancer cells. Cancer Res. **62,** 376–380.

LUTTICKEN, C., WEGENKA, U.M., YUAN, J., BUSCHMANN, J., SCHINDLER, C., ZIEMIECKI, A., HARPUR, A.G., WILKS, A.F., YASUKAWA, K., TAGA, T., *et al.* (1994). Association of transcription factor APRF and protein kinase Jak1 with the interleukin-6 signal transducer gp130. Science **263,** 89–92.

MAZUMDER A., *et al.* (1996). Inhibition of the human immunodeficiency virus type 1 integrase by guanosine quartet structures. Biochemistry **35,** 13762–13771.

MORA, L.B., BUETTNER, R., SEIGNE, J., DIAZ, J., AHMAD, N., GARCIA, R., BOWMAN, T., FALCONE, R., FAIRCLOUGH, R., CANTOR, A., S., *et al.* (2002). Constitutive activation of Stat3 in human prostate tumors and cell lines: Direct inhibition of Stat3 signaling induces apoptosis of prostate cancer cells. Cancer Res. **62,** 6659–6666.

O'SHEA, J.J., GADINA, M., and SCHREIBER, R.D. (2002). Cytokine signaling in 2002: New surprises in the Jak/Stat pathway. Cell **109,** (Suppl), S121–S131.

RANDO, F.R., *et al.* (1995). Suppression of human immunodeficiency virus type 1 activity in vitro by oligonucleotides, which form intramolecular tetrads. J. Biol. Chem. **270,** 1754–1760.

RAZ, R., DURBIN, J.E., and LEVY, D.E. (1994). Acute phage response factor and additional member of the interferon-stimulated gene factor 3 family integrate diverse signals from serine phosphorylation for formation of STAT-promoter complexes. Science **267,** 1990–1994.

SCHINDLER, C., and DARNELL, J.E., Jr. (1995). Transcriptional responses to polypeptide ligands: the JAK-ATAT pathway. Annu. Rev. Biochem. **64,** 621–651.

SEN, D., and GILLBERT, W. (1990). A sodium-potassium switch in the formation of four-stranded G4–DNA. Nature **344,** 410–414.

TURKSON, J., and JOVE, R. (2000). STAT proteins: Novel molecular target for cancer drug discovery. Oncogene **19,** 6613–6626.

TWEARDY, D.J., WRIGHT, T.M., *et al.* (1995). Granulocyte colony stimulating factor rapidly activates a distinct STAT-like protein in normal myeloid cells. Blood **86,** 4409–4416.

VAKSER, I.A. (1996). Long-distance potentials: An approach to the multiple-minima problem in ligand-receptor interaction. Protein Eng. **9,** 37–41.

WEGENKA, U.M., LUTTICKEN, C., BUSCHMANN, J., YUAN, J., LOTTSPEICH, F., MULLER-ESTERL, W., SCHINDLER, C., ROEB, E., HEINRICH, P.C., and HORN, F. (1994). The interleukin-6–activated acute-phase response factor is antigenically and functionally related to members of the signal transducer and activator of transcription (STAT) family. Mol. Cell. Biol. **14,** 3186–3196.

WILLIAMSON, J.R. (1994). G-quartet structures in telemetric DNA. Annu. Rev. Biophys. Biomol. Struct. **23,** 703–730.

ZHONG, Z., WEN, Z., and DARNELL, J.E. (1994). Stat3: A STAT family member activated by tyrosine phosphorylation in response to epidermal growth factor and interleukin-6. Science **264,** 95–98.

ZHOU, P., QIAN, L., KOZOPAS, K.M., and CRAIG, R.W. (1997). Mcl-1, a bcl-2 family member, delays the death of hematopoietic cells under a variety of apoptosis-inducing conditions. Blood **89,** 630–643.

Address reprint requests to:
Naijie Jing, Ph.D.
Section of Infectious Diseases
Department of Medicine
Baylor College of Medicine
Houston, TX 77030

E-mail: njing@bcm.tmc.edu

Received for publication August 8, 2003; received in revised form September 19, 2003; accepted September 24, 2003.

Running title: GQ-ODN as Stat3 inhibitors suppresses tumor growth

G-QUARTET OLIGONUCLEOTIDES: A NEW CLASS OF STAT3 INHIBITORS THAT SUPPRESSES GROWTH OF PROSTATE AND BREAST TUMORS THROUGH INDUCTION OF APOPTOSIS

Naijie Jing*, Yidong Li, Weijun Xiong, Wei Sha, Ling Jing[ϕ], David J. Tweardy

Department of Medicine, Section of Infectious Diseases,

Baylor College of Medicine, Houston TX 77030;

[ϕ] University of Texas Health Science Center,

School of Public Health, Houston TX77030

*To whom correspondence should be addressed

Phone 713-798-3685

Fax 713-798-8948

E-mail: njing@bcm.tmc.edu

Key words: 1. GQ-ODN: G-quartet forming oligodeoxynucleotide. 2. Stat3: Signal transducer and activator of transcription 3. 3. Apoptosis. 4. Anti-cancer drug. 5. Drug delivery.

ABSTRACT

Stat3 is a signaling molecular and oncogene activated frequently in many human malignancies including the majority of prostate, breast and head and neck cancers; yet, no current chemotherapeutic approach has been implemented clinically that specifically targets Stat3. We recently developed G-rich oligodeoxynucleotides, which form intramolecular G-quartet structures (GQ-ODN), as a new class of Stat3 inhibitor. GQ-ODN targeted Stat3 protein directly inhibiting its ability to bind DNA. When delivered into cells using polyethyleneimine (PEI) as vehicle, GQ-ODN blocked ligand-induced Stat3 activation and Stat3-mediated transcription of anti-apoptotic genes. To establish the effectiveness of GQ-ODN as a potential new chemotherapeutic agent, we systemically administered GQ-ODN plus PEI or PEI alone (placebo) by tail vein injection into nude mice with prostate and breast tumor xenografts. While the mean volume of breast tumor xenografts in placebo-treated mice increased by 6.7 fold over 18 days, xenografts in the GQ-ODN-treated mice remained unchanged ($p=0.006$). Similarly, while the mean volume of prostate tumor xenografts in placebo-treated mice increased 9 fold over 10 days, xenografts in GQ-ODN-treated mice increased by only 2.2 fold ($p=0.001$). Biochemical and histological examination of tumors from mice treated with G-quartet ODN demonstrated a 9-fold reduction in Stat3 activation, a reduction in levels of the anti-apoptotic proteins Bcl-2 and Bcl-x_L of 4 fold and 10 fold, respectively, and a 8-fold increase in the number of apoptotic cells compared to the tumors of placebo-treated mice. Thus, GQ-ODN targeting Stat3 induce tumor cell apoptosis when delivered into tumor xenografts following intravenous injection and represent a novel class of chemotherapeutic agents that holds promise for the systemic treatment of many forms of metastatic cancer.

INTRODUCTION

Signal transducer and activator of transcription (STAT) proteins were originally discovered as latent cytoplasmic transcription factors (1). STAT proteins, including Stat1, 2, 3, 4, 5a, 5b and 6, link to a variety of cellular and biological processes including proliferation, differentiation, apoptosis, host defense and transformation (2-6). STAT proteins are localized within the cytoplasm of resting cells and become activated by tyrosine phosphorylation at their C-terminal end (Y705) following recruitment to activated receptor complexes. Tyrosine phosphorylation induces formation of dimers, which translocate to the nucleus, where they bind to DNA-response elements in the promoters of target genes and activate transcription (7).

Stat3, previously termed acute phase response factor (APRF) (8-11), is activated within cells by binding to the cell surface of over 40 ligands; it also is constitutively activated in many human cancers (12-14) including 82% of prostate cancers (15), 69% of breast cancers (16), 82-100% of squamous cell carcinoma of head and neck (SCCHN) (17) and 71% of nasopharyngeal carcinoma (18). Activated Stat3 up-regulates the expressions of anti-apoptosis proteins, such as Bcl-x_L and Mcl-1, thereby decreasing spontaneous apoptosis in cancer cells (19, 20). Targeting of Stat3 directly with agents, such as antisense oligonucleotides (21-23), a decoy oligonucleotide (24), or indirectly with JAK inhibitors, AG490 and JSI-124 (25, 26), demonstrated that Stat3 activation contributes to tumor cell growth and resistances to apoptosis, providing the strongest rationale for therapeutic approaches aimed at reducing levels or activity of Stat3 in cancers where it is activated.

Stat3, similar to all STAT proteins, is composed of several domains: a tetramerization domain, a coil-coil domain, a DNA-binding domain, a linker domain, an SH2 domain, a critical tyrosine reside

(Y705), and a C-terminal transactivation domain. Resolution of the crystal structure of Stat3 revealed the structural basis for DNA-binding and dimer formation in sufficient detail to provide primary targets for novel drug development (27). One class of drug in early development as a novel agent targeting Stat3 are G-rich oligodeoxynucleotides (ODN) that form G-quartet structures intracellularly (28).

G-rich DNA and RNA have the ability to form inter- and intramolecular four-stranded structures, referred to as G-quartets (29, 30). G-quartets arise from the association of four G-bases into a cyclic Hoogsteen H-bonding arrangement and each G-base makes two H-bonds with its neighbor G-base (N1 to O6 and N2 to N7). G-quartets stack on top of each other to give rise to tetrad-helical structures. The stability of G-quartet structures depends on several factors: the presence of the monovalent cations, the concentration of the G-rich oligonucleotides present, and the sequence of the G-rich oligonucleotides under study. Potassium with the optimal size to interact within a G-octamer greatly promotes the formation of G-quartet structures and increases their stability. GQ-ODNs have been suggested to play a critical role in several biological processes including modulation of telomere activity (31), inhibition of human thrombin (32), HIV infection (33), HIV-1 integrase activity (34-36), human nuclear topoisomerase 1 activity (37) and DNA replication *in vitro* (38). Based upon the structure and mechanism of Stat3 activation, G-quartet forming oligonucleotides were recently developed to block Stat3 activity within cancer cells (28). G-quartet oligodeoxynucleotides (GQ-ODNs) directly target Stat3 protein and inhibit their ability to bind DNA thereby decreasing transcriptional activation of genes important for apoptosis resistance, such as Bcl-x and Mcl-1.

In the present report, we demonstrated that intravenous administration of GQ-ODNs dramatically reduces the growth in nude mice of xenografts of prostate and breast cancer cells in which Stat3 is

constitutively activated. GQ-ODNs inhibited tumor cell growth by markedly enhancing tumor cell apoptosis and represent a promising agent for treatment of metastatic tumors in which Stat3 is constitutively activated.

MATERIALS AND METHODS

Materials. All G-rich ODNs including 5'-fluorescein-labeled ODN were synthesized by Midland Certified Reagent Company (Midland, Texas) and used without further chemical modifications. The human cell lines HepG2, PC-3 and MDA-MB-468 were obtained from the ATCC. Polyethylenimine (PEI, ~25 kD polymer, Aldrich Chemical, WI) was generously provided by Dr. Charles Densmore (Baylor College of Medicine). Interleukin 6 (IL-6) and antibodies against Stat3, Stat1, Bcl-x_L and Bcl-2 were purchased from Santa Cruz Biotech. Inc. Antibody against Caspase 3 was obtained from Cell Signaling Technology.

Assay of inhibition by GQ-ODNs of Stat3 DNA-binding activity in cancer cells. GQ-ODN plus PEI at a weight ratio of PEI/ODN of 2:1 was added to cells ($5\text{-}7x10^5$). After incubation for 3 hours, the cells were washed three times with fresh medium without PEI/ODN and the incubation continued. After 6 to 72 hours, cells were incubated without or with IL-6 (25ng/mL) at 37°C for 20 minutes before extraction and analysis by electrophoretic mobility shift assay (EMSA). The cell extraction and EMSA were performed as described previously (28). In some experiments, cells were scraped and harvested for isolation of nuclear proteins as described previously (39). Briefly, 50 µl of ice-cold Buffer A (10mM Tris-HCL pH 9, 2mM $MgCl_2$, 5mM KCl, 10% glycerol, 1mM EDTA, 1mM DDT) plus 1% NP40 was added and the cells allowed to swell on ice for 15 minutes, then vortexed vigorously. The lysate was centrifuged at 700g for 5 minutes at 4°C and the resulting nuclear pallet resuspended in 50µl of cold buffer (20mM HEPES, 0.4M NaCl, 1mM EDTA, 1mM EGTA, 1mM

DDT). Nuclear proteins were extracted by vigorous shaking for 30 minutes at 4°C and cell debris pelleted by centrifugation at 18,000g for 5 minutes at 4°C. Protein concentrations of whole-cell and nuclear extracts were measured by Bradford assay.

Statistical docking calculations. The structures of the designed G-quartet ODNs, such as T40214 and its analogs, were built up through modification of the NMR structure of GQ-ODN T30923 (40) and optimized under AMBER force field by INSIGHTII/DISCOVER. The optimization of the molecular structures proceeded as follows: (1) 100 steps of conjugate gradient energy minimization, (2) 1,000 steps of restrained MD equilibration with a time step of 0.33 fs at 1000K, (3) 1,000 steps of restrained MD equilibration with a time step of 0.1 fs at 300K and (4) 1,000 steps of conjugate gradient energy minimization. The intramolecular H-bonds of G-quartets were used as constraints for the molecular optimization.

We docked each GQ-ODN one thousand times onto the available structure of the dimer of Stat3 SH2 (27) using the GRAMM docking program without placing any restrictions on binding sites. This program uses a geometry-based algorithm for predicting the structures of complexes between molecules of known structure. It can provide quantitative data related to the quality of the contact between the molecules. The intermolecular energy calculation relies on the well-established correlation and Fourier transformation techniques used in the field of pattern recognition. The distribution of H-bond formation between each Stat3/GQ-ODN complex were calculated and analyzed.

***In vivo* delivery of fluorescently labeled GQ-ODN.** Fluorescent labeled T40214 plus PEI (each 2.5mg/kg) were injected into the tail vein of male and female mice weighing approximately 20g.

Twenty-four hours after the infusion, the mice were sacrificed and tissue harvested and frozen. Frozen tissues were sectioned using a cryostat microtome sections, lightly fixed and viewed microscopically.

Tumor xenograft models. Athymic nude mice (Balb/nu/nu, four weeks old and weighing ~20g obtained from Charles River Labs) were injected subcutaneously into the right (or left) flank with one million cancer cells (MDA-MD-468 or PC-3) in 200 µl PBS. After tumors were established at 7 to 14 days post-injection, sixteen nude mice with breast or prostate tumors were randomly assigned into two groups. Mice in Group 1 (n=7) served as placebo and received only PEI (2.5 mg/kg) while mice in Group 2 (n=7) received T40214 (5.0 mg/kg) plus PEI (2.5 mg/kg). Treatments, administered by tail vein injection, and sizing of tumors occurred every two days. The unpaired two-sample t-test, $[t=(X_1-X_2)/S_p^2(1/n_1+1/n_2))^{1/2}]$, was used to determine differences in tumor sizes between the placebo and the drug-treated groups.

Immunoblotting. Tumor xenografts were harvested at the end of treatment period, cut into small pieces, homogenized on ice for 2 minutes, subjected to one round of freeze-thawing and centrifuged (12,000 rpm for 2 min at 4°C). The supernatants were harvested, assayed for protein concentration by Bradford assay and immunoblotted as described elsewhere (21).

TUNEL assay. The terminal deoxynucleotidyl transferase (TdT)-mediated dUTP-biotin nick end-labeling (TUNEL) assay was performed as described by the manufacturer (Roche Applied Science). Briefly, prostate (or breast) tumors were harvested from mice within 24 hours of their last treatment. The paraffin-embedded tissues were pretreated using Xylene and ethanol, washed with PBS and incubated with proteinase K working solution. TUNEL reaction mixture was prepared by adding 50µl of enzyme solution into 450µl of the labeling solution. TUNEL reaction mixture (50µl) was

placed on slides followed by 50μl DAB substrate. Slides were incubated for 5 minute at 24°C, rinsed 3 times with PBS, dehydrated with Xylene and mounted under a glass coverslip.

RESULTS

Inhibition of Stat3 activation by G-quartet ODNs in cancer cells.

Stat3 is expressed and constitutively activated in the prostate cancer cell line, PC-3, and the breast cancer cell line, MDA-MB-468 (25, 41). The GQ-ODN T40214 and a panel of related G-rich ODNs capable of forming G-quartets were mixed with PEI and each were examined for the ability to inhibit Stat3 activation in these cell lines (Figure 1A-C; Table 1). Each of the G-rich ODN demonstrated the ability to inhibit Stat3 DNA-binding activity when the concentration of ODN was increased from 7 to 285 μM. T40214 was the most potent at inhibiting Stat3 activation. Non-specific ODN (ns-ODN) incapable of forming the G-quartet structure demonstrated no activity against Stat3.

Structure-activity relationship between Stat3 and G-quartet inhibitors.

T40214 was previously determined to form an intramolecular G-quartet structure composed of two G-quartets in the center and two G-C-G-C loop domains on the top and bottom with approximately 15Å width and 15Å length (40, 42). T40214 and other GQ-ODN destabilize Stat3 dimers by inserting between their SH2 domains. We proposed that GQ-ODN interact in the region of the SH2 domain from amino acid residues 638 to 650 (28; Figure 2A). To establish a structure-activity relationship between Stat3 and G-quartet inhibitors, we generated the G-quartet structure predicted to be formed by each G-rich ODN (Table 1) and randomly docked each of them onto the known structure of the dimer of Stat3 SH2 domains (27) one thousand times. Analysis of the histogram of H-bonds formed at each residue within the Stat3 SH2 domain demonstrated that T40214 interacts with SH2 predominantly in the region from residues 638 to 650, as expected, with 35% of total H-bonds formed

located in this region (Figure 2B). The percentages of H-bonds formed within the region from residues 638 to 650 of Stat3 for other GQ-ODNs were listed in Table 1. Composite analysis of all histograms revealed that there is an inverse linear correlation between the percentage of GQ-ODN H-binding within this region of the Stat3 SH2 domain and the IC_{50} of inhibition of Stat3 DNA binding activity (Figure 2C). Thus, these findings indicate that the higher the percentage of GQ-ODN H-bond formation within this region of Stat3 SH2, the greater its ability to inhibit Stat3 activation within cells.

GQ- ODN-mediated inhibition of Stat3 within cells is selective for Stat3, requires PEI and is accompanied by decreased levels of intranuclear Stat3 phosphorylated on Y705 (Stat3-pY705).

We previously demonstrated that GQ-ODN had 4-fold greater activity against Stat3 than Stat1 *in vitro* (28). To determine if this selectively persisted or increased upon intracellular delivery, we pre-incubated HepG2 cells, in which both Stat3 and Stat1 are activated by IL-6, with T40214 (0-142 μM) for 72 hr before stimulation with IL-6. Pre-incubation of HepG2 cells with T40214/PEI complex at 70 μM (or higher) nearly completely inhibited IL-6-mediated activation of Stat3 while activation of Stat1 was only mildly affected (Figure 3A and C) confirming the selectivity of GQ-ODN for Stat3 within cells. No inhibition of Stat3 DNA binding activity was observed when HepG2 cells were pre-incubated with T40214 in the absence of PEI (Figure 3B) confirming previous findings by us (40) that a vehicle is required for delivery of GQ-ODN into cells.

To determine if GQ-ODN also interfere with Stat3 activation and translocation into the nucleus, we examined levels of Stat3-pY705 within the nucleus of cells stimulated with IL-6 following GQ-ODN pre-treatment. Levels of Stat3-pY705 were reduced from 50 to 70% in nuclei when the concentration of T40214 was increased from 3.5 to 142 μM (Lane from 4 to 7 in Figure 4). PEI alone as vehicle has no effect on Stat3 activation (Lane 3).

Delivery of G-quartet ODN into tumor xenografts results in inhibition of growth through induction of apoptosis.

To determine if GQ-ODNs can be administered to mice and delivered into tumor xenografts, we injected fluorescein-labeled T40214 plus PEI (each at 2.5mg/kg) into the tail veins of nude mice with established tumor xenografts. Microscopic examination of xenografts 24 hours after injection demonstrated diffuse fluorescent staining within tumor cells (Figure 4A) indicating that GQ-ODN enters and accumulates within tumor cells.

To assess if GQ-ODN uptake is accompanied by inhibition of tumor growth, nude mice were injected subcutaneously with PC-3 or MDA-MB-468, both of which demonstrate constitutive Stat3 activity, and intravenously treated every other day after tumors were established. One group (n=7) received T40214 (5.0 mg/kg) plus PEI (2.5 mg/kg) and the other group (placebo, n=7) received PEI (2.5 mg/kg) alone by tail vein injection. The mean size of the prostate tumor xenografts of placebo-treated mice increased by 9 fold while that of the drug-treated mice increased by only 2.2 fold ($p=0.001$) (Figure 4B & C). Similarly, the mean size of the breast tumor xenografts of placebo-treated mice increased 6.7 fold while that of drug-treated mice remained unchanged ($p=0.006$) (Figure 4D).

To gain insight into the mechanism of inhibition of tumor growth by GQ-ODN, we harvested the prostate tumor xenografts from placebo-treated and drug-treated mice after five treatments and extracted proteins to assess for levels of Stat3-pY705, Bcl-x_L, Bcl-2 and activated Caspase 3 protein. Levels of Stat3-pY705, Bcl-x_L and Bcl-2 were decreased by 9, 4.3 and 10-fold, respectively, in the tumors from drug-treated animals compared to tumors from placebo-treated mice. These changes

were accompanied by a 3-fold increase in Caspase 3 cleavage products in the tumors from drug-treated animals compared to tumors from placebo-treated mice (Figure 6A). We have harvested the 4 tumor samples from placebo-treated mice and 3 tumor samples from drug-treated mice and then performed TUNEL assay on the samples. TUNEL staining was performed on 4 tumor samples from placebo-treated mice and 3 tumor samples from drug-treated mice to assess if GQ-ODN treatment increased tumor cell apoptosis. The percentage of apoptotic cells was reduced nearly 8-fold in the tumors of drug-treated mice (83.6 ± 1.0%) compared to the tumors of placebo-treated mice (11.2 ± 10.1%. $P<0.001$) (Figure 6B and Table 2).

DISCUSSION

Mounting evidence from cell culture, whole animals and patient samples indicates that Stat3 is a critical mediator of oncogenic signaling that is activated in many human malignancies (18). This evidence provides a strong rationale for developing agents that target Stat3 for treatment of cancers in which constitutive Stat3 activation plays a critical role. Currently, no chemotherapeutic approach has been implemented that targets Stat3. We recently developed G-rich oligodeoxynucleotides, which form intramolecular G-quartet structures (GQ-ODN), as a new class of Stat3 inhibitor; GQ-ODN were shown to target Stat3 dimers predominantly in the regions of their SH2 domains resulting in their destabilization and reduced ability to bind DNA *in vitro* (28). In studies reported here, we demonstrate that when delivered into cells using polyethyleneimine (PEI) as vehicle, GQ-ODN blocked ligand-induced Stat3 activation. We determined that the region within the SH2 dimer domains predominantly bound by GQ-ODN was located between residues 638 and 650, a region critically involved in Stat3 dimerization. Importantly, we established a linear structure-activity relationship that directly correlates the ability of a GQ-ODN to bind to this region of Stat3 SH2 and its ability to inhibit Stat3 activation within cells, which is an important step towards optimizing the

design GQ-ODN inhibitors of Stat3. Furthermore, intravenous administration of GQ-ODN plus PEI blocked the growth of breast and prostate tumor xenografts in nude mice. This effect was accompanied by marked reductions in levels of Stat3 activation and Bcl-2 and Bcl-x_L protein and a striking increase in tumor cell apoptosis. Thus, GQ-ODN, which target Stat3 and induce apoptosis within tumor xenografts following intravenous administration, represent a novel cancer chemotherapeutic approach that holds promise for the systemic treatment of many forms of metastatic cancer.

Our previous studies showed that the G-quartet structure of G-rich ODN is essential for the inhibition of Stat3 DNA-binding activity *in vitro* (28). The G-quartet structure of T40214 closely resembles a perfect cylinder 15 Å in width and length. This conformation increases the thermal stability of the structures, reduces the capacity of ODN to form molecular aggregates, and increases the probability that each GQ-ODN will target Stat3 homedimer in cells. The finding that T40214-mediated inhibition of ligand-induced Stat3 activation within cells persisted for 72 hours after GQ-ODN exposure can be attributed, in part, to this compact configuration, which contributes to its thermal stability and resistance to nuclease digestion. The intramolecular G-quartet structure prevents single-strand endonucleases from accessing their cleavage sites (43).

Effective delivery of GQ-ODNs into cancer cells is a key factor for success of inhibitors that target oncogenic signaling intermediates. On the basis of the property of potassium-dependent formation of G-quartet structure, a novel intracellular delivery system has been developed for GQ-ODNs (42). Using the novel delivery system, GQ-ODNs were delivered efficiently into the cytoplasm and nucleus of cells. The results reported here showed that GQ-ODNs penetrated poorly into cells without vehicle as evidenced by low drug activity while use of an effective intracellular delivery system such as PEI

increased the drug activity of GQ-ODNs in cancer cells (Figure 3A & B). When G-rich ODNs form intramolecular G-quartet structures within the cytoplasm, they are able to diffuse freely through pores into the nucleus, bind to Stat3 and block the transcription of Stat3 regulated genes (Figure 4) (28).

Because of the important role that STAT proteins play in signaling within the immune system (Stat1, 2, 4, 5A, 5B and 6) and in negative regulation of proliferation (Stat1) (44), it is highly desirable that an agent targeting Stat3 not have activity against other STAT proteins in order to avoid problems with immunosuppression and inadvertent stimulation of tumor cell growth. On the basis of their structures (15, 45), the ligand-receptor pairs that lead to their activation (1) and the phosphotyrosine sites that lead to their recruitment and activation (46), the STAT protein family member that most closely resembles Stat3 is Stat1. Stat3 and Stat1 share greater than 50% amino acid sequence homology in the region of the SH2 domain (15). Therefore, to address the issue of specificity of GQ-ODN inhibition, we focused on Stat1. In previous studies, we demonstrated that the IC_{50} of T40214 for the inhibition of Stat3 DNA-binding activity *in vitro* was four-fold less than for its inhibition of Stat1 DNA-binding activity (26). Here, we demonstrated that the specificity of T40214 for Stat3 vs. Stat1 extends *in vivo*. The concentration of T40214 that inhibited 50% of Stat3 activation after pre-incubation of T40214 in cells was ~11 μM (Figure 3C), while 50% inhibition of Stat1 under the same conditions could not be achieved with concentrations of T40214 up to142 μM. The basis for this selectivity was explained, in part, by the analysis of histograms, which were generated by docking the structure of T40214 onto the structures of Stat3β and Stat1 homodimers two thousand times without setting any binding site restrictions (28). These Studies demonstrated that interactions of GQ-ODN with Stat3 were concentrated within the SH2 and DNA-binding domains, in contrast, interactions of GQ-ODN with Stat1 were distributed more broadly over the whole structure of Stat1.

Intravenous administration of GQ-ODN plus PEI was well tolerated by mice at the dose used in this study. Detailed toxicity studies are in progress; however, toxicity studies of GQ-ODN T30177, an analog of T40214 that inhibits HIV-1 integrase, has been performed previously (47). T30177 did not induce genetic mutations in three assays—the *Ames*/Salmonella mutagenesis assay, the CHO/HGPRT mammalian cell mutagenesis assay and the mouse micronucleus assay. Acute toxicity studies in mice revealed an LD_{50} for T30177 of 1.5g/kg body weight; chronic toxicity studies in mice following multiple doses did not cause delayed mortality or changes in serum chemistry, hematological parameters or organ histology until the dose of T30177 reached 600 mg/kg, 120 times the dose (5 mg/kg) used in our studies.

The results of *in vivo* drug testing revealed that GQ-ODN T40214 dramatically suppressed the growth of xenografts of prostate and breast cancer cells in which Stat3 is constitutively activated. GQ-ODN T40214 markedly decreased the level of phosphorylated Stat3 in tumor xenografts; this decrease was associated with decreased levels of Bcl-2 and Bcl-x_L protein. Bcl-2 and Bcl-x_L are anti-apoptosis proteins that have ion channel activity, which inhibit the release from mitochondria of cytochrome C (48, 49). Reduced levels of Bcl-2 and Bcl-x_L in tumor xenografts would result in increased release of cytochrome C resulting in activation of the caspase cascade, which includes Caspase 3, leading to cell apoptosis. There was a striking increase in Caspase 3 cleavage products in the tumors of T40214-treated animals that was accompanied by an increase in tumor cell apoptosis of similar magnitude. Our results indicate that GQ-ODNs such as T40214 block tumor xenograft growth by targeting Stat3 and inhibiting its phosphorylation, which blocks the transcription of the anti-apoptosis proteins and triggers the apoptosis of cancer cells. Thus, GQ-ODN represents a novel and potentially promising drug for treatment of metastatic tumors in which Stat3 is constitutively activated as either a single agent or part of a combination regimen.

ACKNOWLEDGMENTS

This work was supported by DOD Award PC020407, NIH grants GM60153 and CA86430.

REFERENCES

1. Darnell Jr., J.E. STATs and gene regulation. *Science* 277, 1630-1635 (1997).

2. Zhong, Z., Wen, Z. and Darnell Jr., J.E. Stat3: a STAT family member activated by tyrosine phosphorylation in response to epidermal growth factor and interleukin-6. *Science* 264, 95-98 (1994).

3. Bromberg J.F., Horvath C.M., Wen Z., Schreiber R.D. and Dannell Jr., J.E. Transcriptionally active Stat1 is required for the antiproliferative effects of both interferon alpha and interferon gamma. *Proc. Natl. Acad. Sci. USA* 93, 7673-7678 (1996).

4. Fukada, T., Hibi, M., Yamanaka, Y., Takahashi-Tezuka, M., Fujitani, Y., Yamaguchi, T., Nakajima, K. and Hirano, T. Two signals are necessary for cell proliferation induced by a cytokine receptor gp130: involvement of STAT3 in anti-apoptosis. *Immunity* 5, 449-460 (1996).

5. Planas, A.M., Berruezo, M., Justicia, C., Barron, S. and Ferrer, I. Stat3 is present in the developing and adult rat cerebellum and participates in the formation of transcription complexes binding DNA at the sis-inducible element. *J. Neurochem* 68, 1345-1351 (1997).

6. Takeda, K., Noguchi, K., Shi, W., Tanaka, T., Matsumoto, M., Yoshida, N., Kishimoto, T. and Akira, S. Targeted disruption of the mouse Stat3 gene leads to early embryonic lethality. *Proc. Natl. Acad. Sci. USA* 94, 3801-3804 (1997).

7. Bromberg, J. and Darnell, J.E. The role of STATs in transcriptional control and their impact on cellular function. *Oncogene* 19, 2468-2473 (2000).

8. Wegenka, U.M., Lutticken, C., Buschmann, J., Yuan, J., Lottspeich, F., Muller-Esterl, W., Schindler, C., Roeb, E., Heinrich, P.C. and Horn, F. The interleukin-6-activated acute-phase response

factor is antigenically and functionally related to members of the signal transducer and activator of transcription (STAT) family. *Mol. Cell. Biol.* 14, 3186-3196 (1994).

9. Lutticken, C., Wegenka, U.M., Yuan, J., Buschmann, J., Schindler, C., Ziemiecki, A., Harpur, A.G., Wilks, A.F., Yasukawa, K., Taga, T., et al. Association of transcription factor APRF and protein kinase jak 1 with the interleukin-6 signal transducer gp130. *Science* 263, 89-92 (1994).

10. Zhong, Z., Wen, Z., and Darnell, J.E. Stat3: a STAT family member activated by tyrosine phosphorylation in response to epidermal growth factor and interleukin-6. *Science* 264, 95-98 (1994).

11. Raz, R., Durbin, J.E., and Levy, D.E. Acute phage response factor and additional member of the interferon-stimulated gene factor 3 family integrate diverse signals from cytokines, interferons, and growth factor. *J. Biol. Chem.* 269, 24391-24395 (1994).

12. Bowman, T., Garcia, R., Turkson, J. and Jove, R. STATs in oncogenesis. *Oncogene* 19, 2474-2488 (2000).

13. Bromber, J.F. Activation of STAT proteins and growth control. *BioEssay* 23, 161-169 (2001)..

14. Buettner, R., Mora, L.B. and Jove, R. Activated STAT signaling in human tumor provides novel molecular targets for therapeutic intervention. *Clin. Cancer Res.* 8, 945-954 (2002).

15. Mora L. B., Buettner R., Seigne J., Diaz J., Ahmad N., Garcia R., Bowman T., Falcone R., Fairclough R., Cantor A., Muro-Cacho C., Livingston S., Karras J., Pow-Sang J., and Jove R. Constitutive activation of Stat3 in human prostate tumors and cell lines: direct inhibition of Stat3 signaling induces apoptosis of prostate cancer cells. *Cancer Research* 62, 6659-6666 (2002).

16. Dolled-Filhart, M., Camp, R. L., Kowalski, D. P., Smith, B. L. and Rimm, D. L. Tissue microarray analysis of signal transducers and activatior of transcription 3 and phospho-state 3 (Tyr705) in node-negative breast cancer shows nuclear localization is associated with a better prognosis. *Clinical Cancer Res.* 9, 594-600 (2003).

17. Nagpal, J. K., Mishra, R., Das, B. R. Activation of Stat3 as one of early events in tobacco chewing-mediated oral carcinogenesis. *Amecrican Cancer Sociaty* 94, 2393-2400.

18. Hsiao, J-R., Jin, Y-T., Tsai, —-T, Shiau, A-L., Wu, C-L. and Su, W-c. Constitutive activation of Stat3 and Stat5 is present in majority of nasopharyngeal carcinoma and correlates with better prognosis. *Britich J. Cancer* 89, 344-349, (2003).

19. Boise, L.H., Gonzalez-Garcia, M., Postema, C.E., Ding, L., Lindsten, T., Turka, L.A., Mao, X. and Nunez, G and Thompson CB. Bcl-x, a bcl-2-related gene that functions as a dominant regulator of apoptotic cell death. *Cell* 74, 597-608 (1993).

20. Zhou, P., Qian, L., Kozopas, K.M. and Craig, R.W. Mcl-1, a bcl-2 family member, delays the death of hematopoietic cells under a variety of apoptosis-inducing conditions. *Blood* 89, 630-643 (1997).

21. Grandis, J. R., Drenning, S. D. et al. (1998). "Requirement of Stat3 but not Stat1 activation for epidermal growth factor receptor- mediated cell growth *in vitro*." *J Clin Invest* 102,1385-1392.

22. Grandis, J. R., Drenning, S. D., Zeng, Q., Watkins, S. C., Melhem, M. F., Endo, S., Johson, D. E., Huang, L., He, Y. and Kim, J. D. Constitutive activation of stat3 signaling abrogates apoptosis in squamous cell carcinogenesis in vivo. *Proc. Natl. Acad. Sci. USA*, 97, 4227-4232 (2000).

23. Barton, B. E. Karras, J. G., Murphy, T. F., Barton, A., and Huang, H. F-S. signal transducer and activatior of transcription 3 (STAT3) activation in prostate cancer: direct Stat3 inhibition induces apoptosis in prostate cancer lines. *Mol. Cancer Ther.* 3,11-20 (2004).

24. Leong, P. L., Andrews, G. A., Johnson, D. E., Dyer, K. F., Xi, S., Mai, J. C., Robbins, P. D., Gadiparthi, S., burke, N. A., Watkins, S. F., and Grandis, J. R. targeted inhibition of Stat3 with a decoy oligonucleotide abrogates head and neck cancer cell growth. *Proc. Natl. Acad. Sci. USA*, 97, 4138-4143 (2003).

25. Burdelya, L., Catlett-Falcone, R., Levitzki, A., Cheng, F., Mora, L. B., Sotomayor, E., Coppola, D., Sun, J. Z., Sebti, S., Dalton, W. S., Jove, R., and Yu, H. Combination therapy with AG-490 and interleukin 12 achieves greater antitumor effects than either agent alone. *Mol. Cancer Therapeutics* 1, 893-899 (2002).

26. Blaskovich, M. A., Sun, J., Cantor, A., Turkson, J., Jove, R., and Sebti, S. M. Discovery of JSI-124 (Cucurbitacin I), a selective janus kinase/signal transducer and activitor of transcription 3 signaling pathway inhibitor with potent antitumor activity against human and murine cancer cells in mice. Cancer Res. 63, 1270-1279 (2003).

27. Becker, S., Groner, B. and Muller, C. Three-dimensional structure of the Stat3β homodimer bound to DNA. *Nature* 394, 145-150 (1998).

28. Jing, N., Li, Y., Xu, X., Li, P., Feng, L., Tweardy, D. Targeting Stat3 with G-quartet oligonucleotides in human cancer cells. *DNA & Cell Biology* 22, 685-696 (2003).

29. Williamson J. R. G-quartet structures in telomeric DNA. *Annu. Rev. Biophys. Biomol. Structure* 23, 703-730 (1994).

30. Gilber D. E. and Feigon J. Multistranded DNA structures. *Current Opinion Structura. Biol.* 9, 305-214 (1999).

31. Sen, D. and Gilbert, W. Formation of parallel four-stranded complexes by guanine-rich motif for meiosis. *Nature* 334, 364-366 (1998).

32. Bock, L.C., Griffin, L.C., Latham, J.A., Vermaas, E.H. and Toole, J.J. Selection of single-stranded DNA molecules that bind and inhibit human thrombin. *Nature* 355, 564-566 (1992).

33. Wyatt, J.R., Vickers, T.A., Roberson, J.L., Buckeit, R.W., Klimkait, T., Debaets, E., Davies, P.W., Rayner, B., Imbach, J.L. and Ecker, D.J. Combinatorially selected guanosine-quartet structure is a potent inhibitor of HIV envelope-mediated cell fusion. *Proc. Natl. Acad. Sci. USA* 91, 1356-1360 (1994).

34. Rando, R.F., Ojwang, J., Elbaggari, A., Reyes, G.R., Tinder, R., McGrath, M.S. and Hogan, M.E. Suppression of human immunodeficiency virus type 1 activity in vitro by oligonucleotides which form intramolecular tetrads. *J. Biol. Chem.* 270, 1754-1760 (1995).

35. Mazumder, A., Neamati, N., Ojwang, J.O., Sunder, S., Rando, R.F. and Pommier, Y. Inhibition of the human immunodeficiency virus type 1 integrase by guanosine quartet structures. *Biochemistry* 35, 13762-13771 (1996).

36. Jing, N., De Clercq, E., Rando, F.R., Pallansch, L., Lackman-Smith, C., Lee, S. and Hogan, M.E. Stability-activity relationships of a family of G-tetrad forming oligonucleotides as potent HIV inhibitors. *J. Biol. Chem.* 275, 3421-3430 (2000).

37. Marchand C., Pourquier P., Laco G. S., Jing N. and Pommier Y. Interaction of human nuclear topoisomerase I with guanosine quartet-forming and guanosine-rich single-stranded DNA and RNA oligonucleotides. *J. Biol. Chem.* 277, 8906-8911 (2002).

38. Xu, X, Hamhouyia, F., Thomas, S. D., Burke, T. J., Girvan, A. C., McGregor, W. G., Tren, J. O., Miller, D. M., and Bates, P. J. Inhibition of DNA replication and induction of — phase cell cycle arrest by G-rich oligonucleotides. *J. Biol. Chem.* 276, 43221-43230 (2001).

39. Schreiber, W. E., Jamani, A. Pudek, M. R. Screening tests for porphobilinogen are insensitive. The problem and its solution. *Am. J. Clin. Pathol.* 92, 644-649 (1989).

40. Jing, N. and Hogan, M.E. Structure-activity of tetrad-forming oligonucleotides as a potent anti-HIV therapeutic drug. *J. Biol. Chem.* 273, 34992-34999 (1998).

41. Buettner, R., Mora, L.B. and Jove, R. Activated STAT signaling in human tumor provides novel molecular targets for therapeutic intervention. *Clin. Cancer Res.* 8, 945-954 (2002).

42. Jing N., Xiong, W., Guan, Y, Pallansch, L. and Wang, S. Potassium dependent folding: a key to intracellular delivery of G-quartet oligonucleotides as HIV inhibitors. *Biochemistry* 41(17), 5397-5403 (2002).

43. Bishop, J.S., Guy-Caffey, J.K., Ojwang, J.O., Smith, S.R., Hogan, M.E., Cossum, P.A., Rando, R.F. and Chaudhary, N. G-quartet motifs confer nuclease resistance to a potent anti-HIV oligonucleotide. *J. Biol. Chem.* 271, 5698-5703 (1996).

44. O'Shea J. J., Gadina M., Schreiber R. D. Cytokine signaling in 2002: new surprises in the Jak/Stat pathway. *Cell* 109, Suppl:S121-21 (2002).

45. Chen, X., Vinkemeier, U., Zhao, Y., Jeruzalmi, D., Darnell, J.E. and Kuriyan, J. Crystal structure of a tyrosine phosphorylated Stat-1 dimer bound to DNA. *Cell* 93, 827-839 (1998).

46. Wiederkehr-Adam, M., Ernst, P., Muller, K., Bieck, E., Gombert, F. O., Ottl, J., Graff, P., Grossmuller, F., Heim, M. H. Characterization of phosphopeptide motifs specific for the Src homology 2 domains of signal transducer and activator of transcription 1 (STAT1) and STAT3. J Biol Chem. 278, 16117-16128 (2003)

47. Wallace, T. L., Gamba-Vitalo, C, Loveday, K. S., and Cossum, P. A. Acute, multipe-dose, and genetic toxicology of AR177, an anti-HIV oligonucleotide. *Toxicol. Sci.* 53, 63-70 (2000).

48. Schendel, S.,L., Xie, Z., Montal, M. O., Matsuyama, S., Montal, M. and Reed, J. C. Channel formation by antiapoptotic protein Bcl-2. *Proc Natl Acad Sci USA* 94, 5113-5118 (1997).

49. Minn, A. J., Velez, P., Schendel, S. L., Liang, H., Muchmore, S. W., Fesik, S. W., Fill, M. and Thompson, C. B. Bcl-x(L) forms an ion channel in synthetic lipid membranes. *Nature* 385, 353-357 (1997).

TABLES

Table 1. IC_{25}, IC_{50} and IC_{75} of ODN for inhibition of IL-6-stimulated Stat3 activation in PC-3 cells and percent of total H-bond formed between ODN and the region of Stat3 SH2 located between amino acid residues 638 and 650.

Compound	5'-sequence	IC_{25} (μM)	IC_{50} (μM)	IC_{75} (μM)	% H-bounds formed within Stat3 (aa 638-650)
Ns-ODN	TGCCGGATCCAAGAGCTACCA	-----	-----	-----	-----
T40214	GGGCGGGCGGGCGGGC	2.5	5.0	24	35
T40212	GGGCGGGTGGGCGGGT	17	35	142	30
T40215	$(GGGGT)_4$	12	49	163	28
T40216	$(GGGGGT)_4$	30	202	-----	----
T40217	GGGGTGGGTGGGTGGGTT	35	64	-----	27
T40228	GCGGGTGGGTGGGTGGGTCG	139	192	244	----
T40229	TAGGGTGGGTGGGTGGGTAT	9	41	248	29
T40230	GTGGGTGGGTGGGTGGGTTG	11	43	-----	28
T40231	GGTGGGTGGGTGGG	4.6	10	49	33
T40232	GGCGGGCGGGCGGG	10	26	62	32
T40233	GGGCGGGTGGGCGG	7.6	34	67	29

Table 2: Percentage of apoptotic cells within prostate tumor xenografts assessed by TUNEL staining.

Tumors mice xenografts samples from nude	Apoptotic cells (C_A)	Total cells (C_T)	Apoptosis (%) C_A/C_T x 100%
Placebo-treated (1)	9	80	11.3
Placebo-treated (2)	6	114	5.3
Placebo-treated (3)	4	147	2.7
Placebo-treated (4)	21	83	25.3
Mean cells apoptosis (%)			11.2 ± 10.1*
Drug-treated (1)	94	114	82.5
Drug-treated (2)	90	110	84.5
Drug-treated (3)	93	111	83.8
Mean cells apoptosis (%)			83.6 ± 1.0*

* Mean ± SD ($P<0.001$).

FIGURE LEGENDS

Figure 1. Inhibition of Stat3 activation in prostate and breast cancer cells by GQ-ODN. (A) Stat3 is activated constitutively and by IL-6 in PC-3 cells. EMSA was performed using extracts of PC-3 cells without (-) and with (+) stimulation with IL-6 (25 ng/ml); extracts were incubated without or with antibodies against Stat1 (Ab1) and Stat3 (Ab3). EMSA was performed using extracts of IL-6-stimulated PC-3 (B) and MDA-MB-468 cells (C) pre-treated with each of a panel of ODN (see Table 1 for sequences). Cells were pre-incubated with the indicated ODN plus PEI at the indicated concentration for 3 hr, washed and incubated in fresh medium for 24 hr and then stimulated with IL-6 (25 ng/ml) before extraction.

Figure 2. Structure-activity relationship (SAR) of GQ-ODNs. (A) Model of T40214 bound to dimers of Stat3 SH2 showing T40214 (blue wire model) interacting with residues Q643, Q644, N646 and N647 of Stat3 dimer (green space-filling model). (B) Histogram of the distribution of all H-bonds formed between T40214 and the SH2 domain of Stat3 in 1,000 computer-simulated dockings. (C) Plot demonstrating the relationship between the percent of GQ-ODN H-bonding localized from residues 638 to 650 and its IC_{50} against Stat3 (Table 1; $r^2 = 0.91$; $P<0.001$).

Figure 3. GQ-ODN selectively target Stat3 within cells and its delivery requires PEI. EMSA of extracts of HepG2 cells stimulated with IL-6 (25 ng/ml) 72 hr after pre-incubation of cells with T40214 at the indicated concentrations complexed with (A) or without (B) PEI. Extracts were incubated with antibodies against Stat1 (Ab1; lane 1) or Stat3 (Ab3; lane 2) to confirm the composition of the homodimer bands. (C) The intensity of the homodimer bands in lanes 4 through 9

of T40214 with PEI (A) were measured by densitometry and plotted as a percent of the band in the untreated lane (0 μM; lane 4).

Figure 4. GQ-ODN inhibit IL-6-mediated increase in intranuclear phosphorylated Stat3. (A) Immunoblot of nuclear extracts of HepG2 cells pre-incubated with media (0), PEI alone (PEI) or T40214 at the indicated concentrations for 3 hr. Cells were then washed and incubated in medium alone for 24 hr before stimulation with IL-6 (25 ng/ml); nuclear extracts were separated by SDS-PAGE and immunoblotted with anti-phosphotyrosine antibody (pY705; top panel) or Stat3 monoclonal antibody (T-Stat3, bottom panel). (B) The p-Stat3 bands were quantitated by densitometry and plotted as the percent of the PEI-pretreated lane (lane 3).

Figure 5. GQ-ODN T40214 is successfully delivered into tumor xenografts and inhibits their growth. (A) Light microscopic (left panel) and fluorescent microscopic (right panel) photomicrographs (each 400x magnification) of a tumor xenograft harvested from a nude mouse 24 hr following tail vein injection with fluorescein-labeled T40214/PEI complex (each at 2.5 mg/kg), showing the uptake of T40214 within tumor cells. (B) Photographs of a representative placebo treated mouse (left panels) and a drug-treated mouse (right panel) taken at the start of treatment (top) and 10 days into treatment (bottom). Prostate (C) and breast (D) cancer cells xenograft volumes were measured at the start of therapy and every other day in mice treated with T40214/PEI complex (open circles; n=7) or with PEI alone (closed circles; n=7). Data plotted are meand ± SEM of each group.

Figure 6. Effect of G-quartet ODN T40214 on apoptosis and levels of apoptosis-related proteins in tumor xenografts. (A) Proteins were extracted from tumor xenografts obtained from 3 placebo-treated mice (lanes 1 to 3) and from 4 drug-treated mice (lane 4 to 7), separated by SDS-PAGE, and

immunoblotted with the antibodies indicated. Each lane was loaded an equal amount of the total Stat3 (T-Stat3) protein as a control. (B) Photomicrographs (400x magnification) of TUNEL stained sections of a prostate tumor xenograft removed on day 10 from a placebo-treated mouse (left panel) and a drug-treated mouse (right panel). Nuclei of apoptotic tumor cells stained brown while nuclei of non-apoptotic tumor cells were unstained (blue).

A.

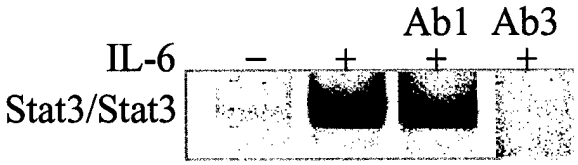
Ab1 Ab3
IL-6 – + + +
Stat3/Stat3

B.

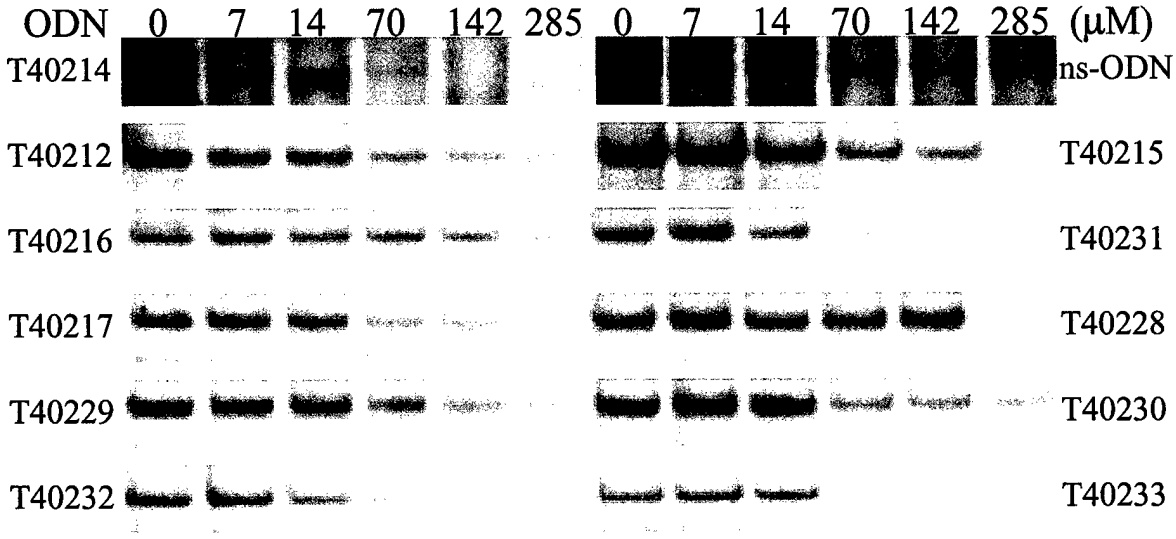
ODN 0 7 14 70 142 285 0 7 14 70 142 285 (μM)
T40214
ns-ODN
T40212
T40215
T40216
T40231
T40217
T40228
T40229
T40230
T40232
T40233

C.

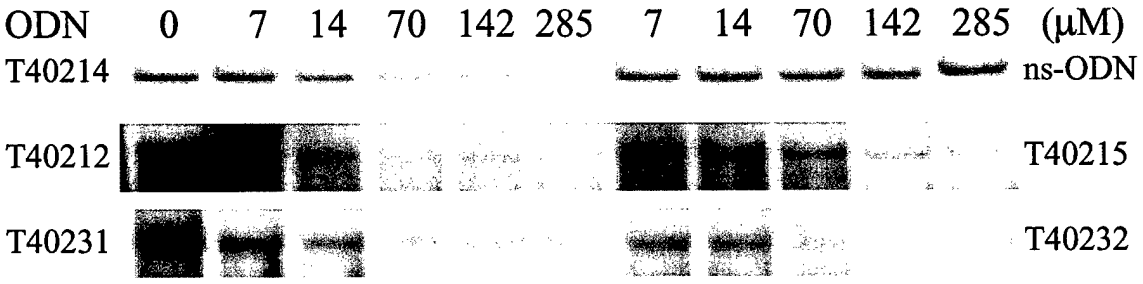
ODN 0 7 14 70 142 285 7 14 70 142 285 (μM)
T40214
ns-ODN
T40212
T40215
T40231
T40232

Figure 1

A.


SH2 Domains

B.

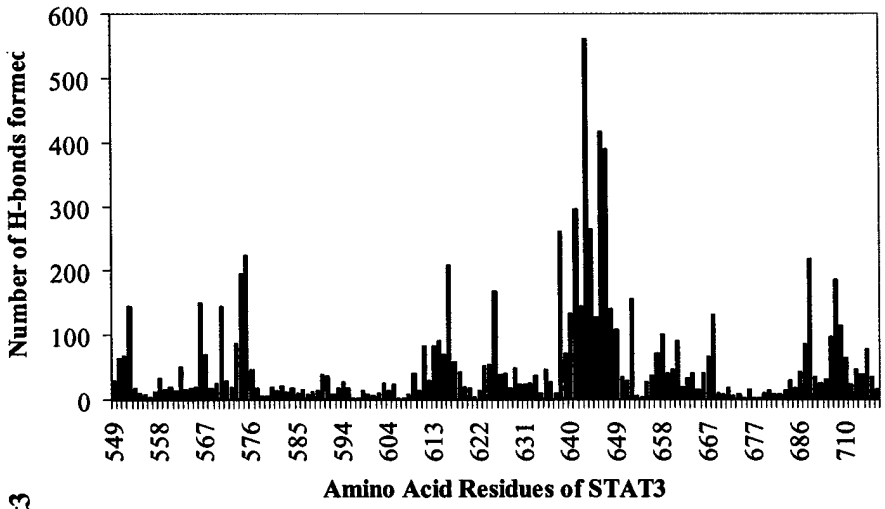
Number of H-bonds formed
600
500
400
300
200
100
0
549
558
567
576
585
594
604
613
622
631
640
649
658
667
677
686
710
Amino Acid Residues of STAT3

C.

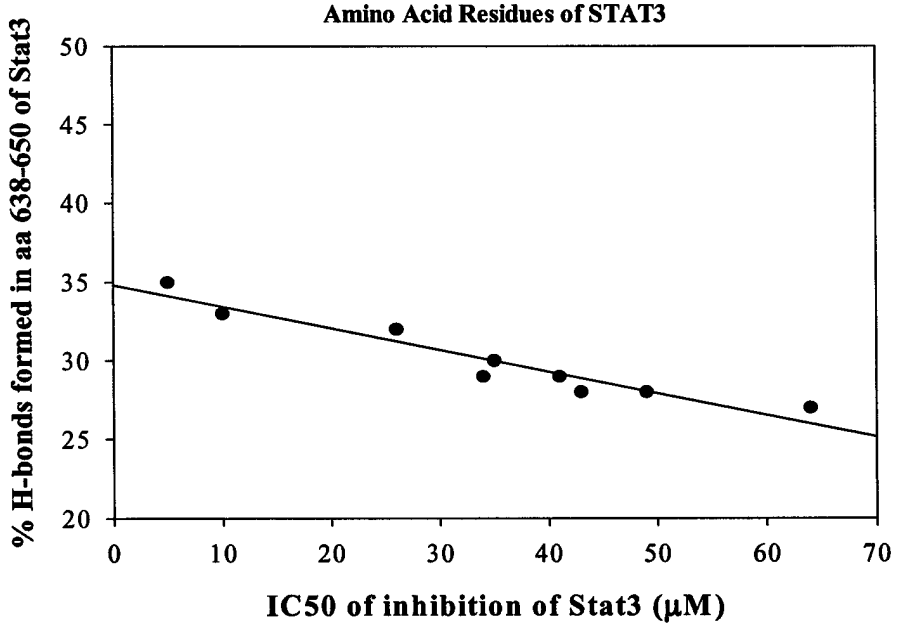
% H-bonds formed in aa 638-650 of Stat3
50
45
40
35
30
25
20
0
10
20
30
40
50
60
70
IC50 of inhibition of Stat3 (μM)

Figure 2

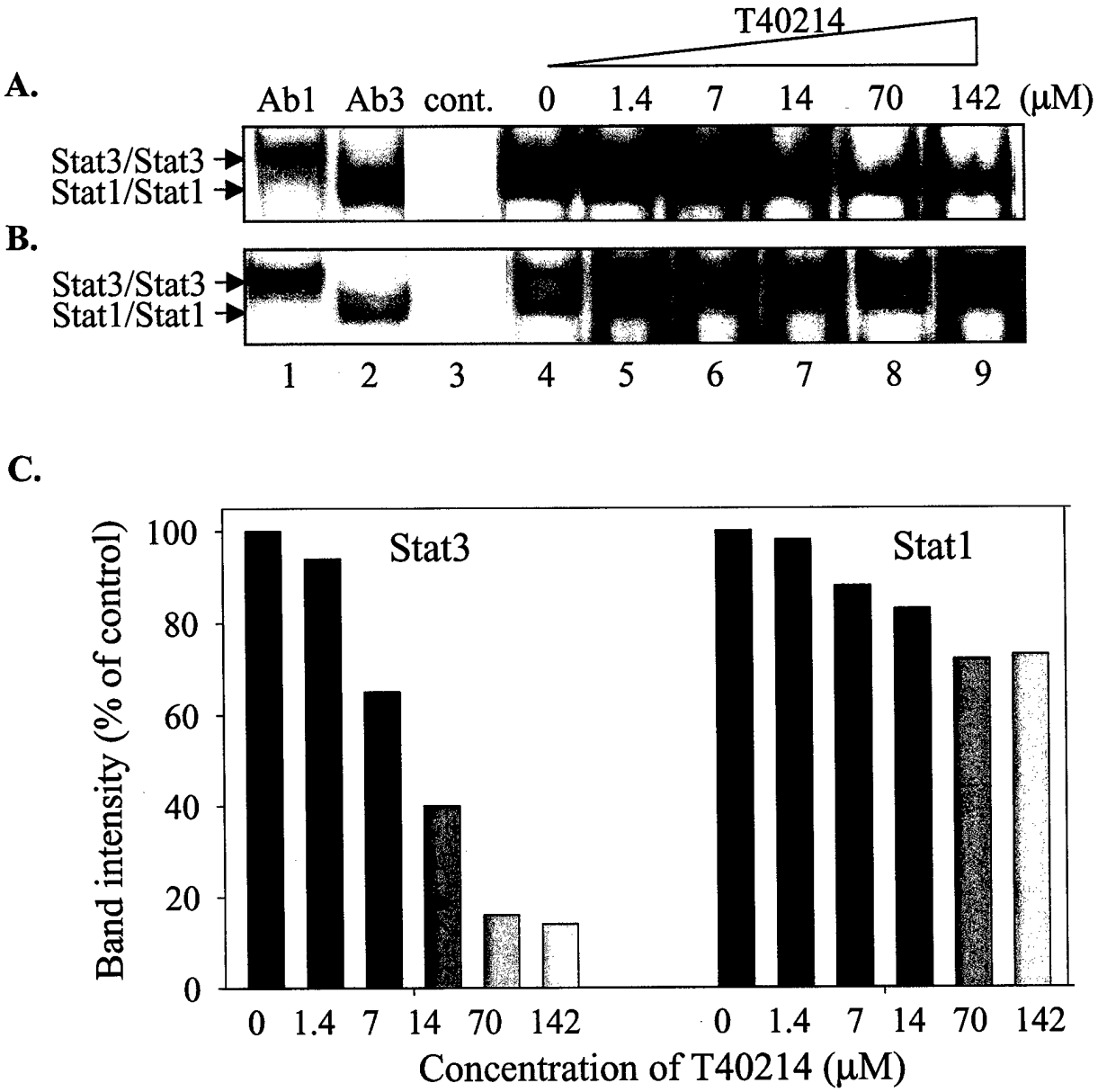
T40214
A.
Ab1 Ab3 cont. 0 1.4 7 14 70 142 (μM)
Stat3/Stat3
Stat1/Stat1
B.
Stat3/Stat3
Stat1/Stat1
1 2 3 4 5 6 7 8 9
C.
Band intensity (% of control)
100
80
60
40
20
0
Stat3
Stat1
0 1.4 7 14 70 142
0 1.4 7 14 70 142
Concentration of T40214 (μM)

Figure 3

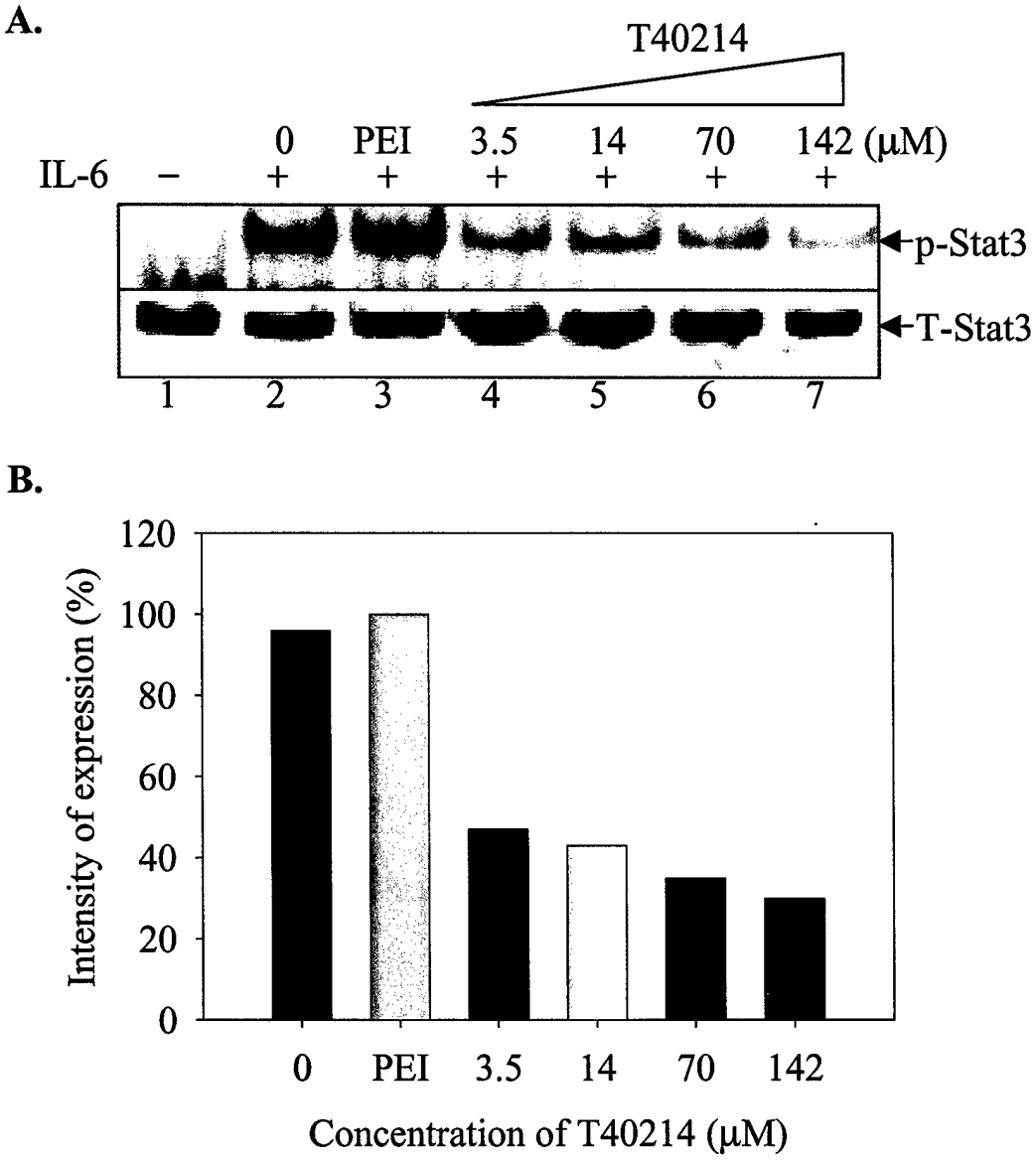
A.
T40214
0
PEI
3.5
14
70
142 (μM)
IL-6
–
+
+
+
+
+
+
p-Stat3
T-Stat3
1
2
3
4
5
6
7
B.
120
100
80
60
40
20
0
Intensity of expression (%)
0
PEI
3.5
14
70
142
Concentration of T40214 (μM)

Figure 4

A.

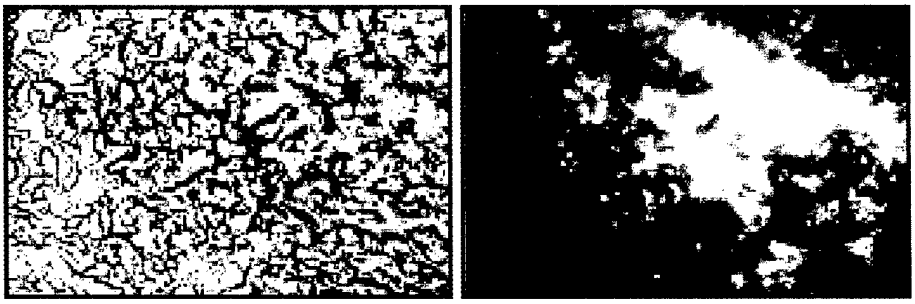

B.

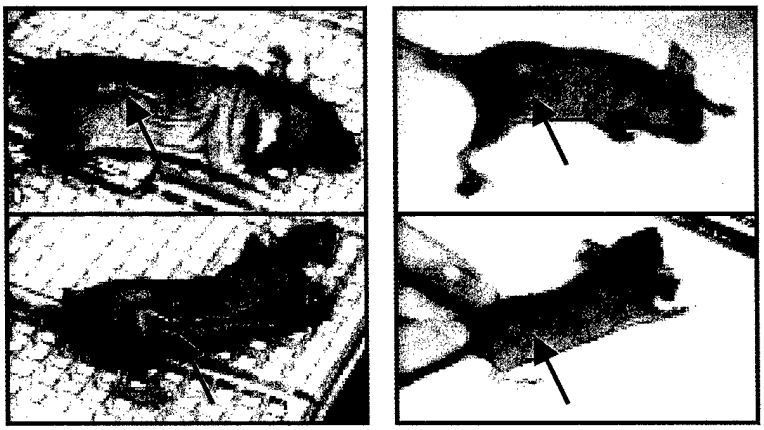

C.

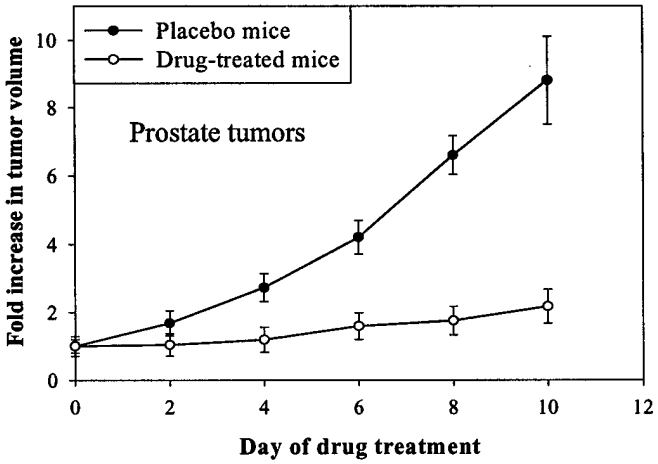

D.

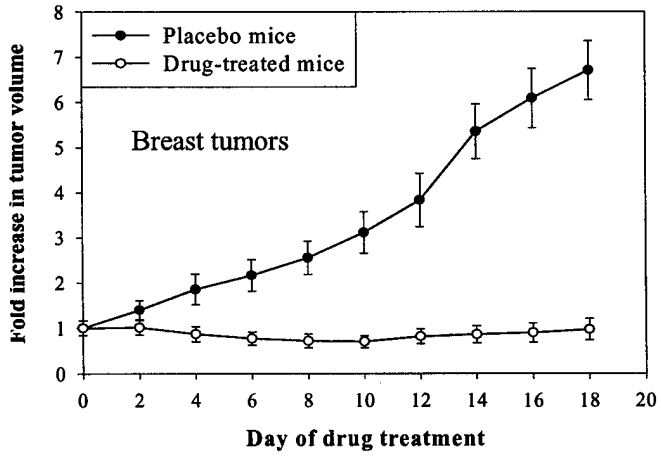

Figure 5

A.

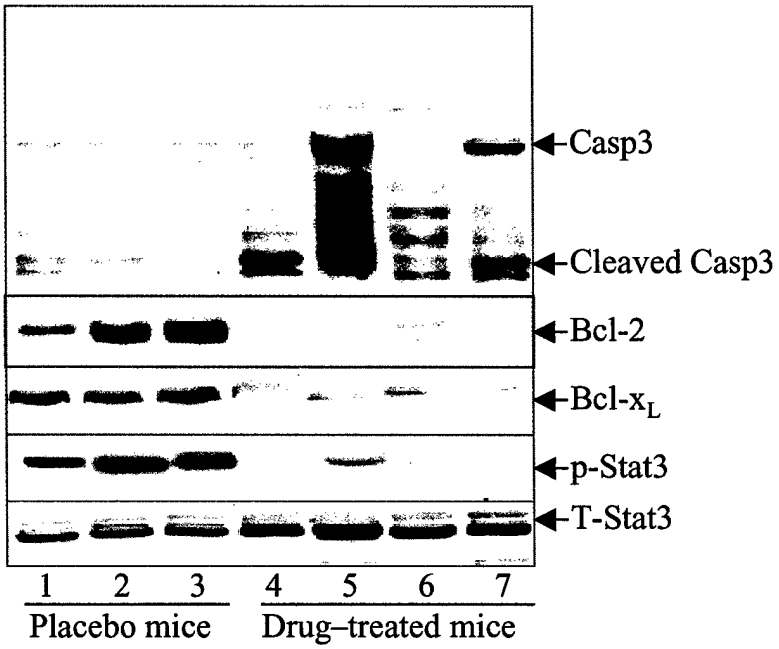
Casp3
Cleaved Casp3
Bcl-2
Bcl-x_L
p-Stat3
T-Stat3
1 2 3 4 5 6 7
Placebo mice
Drug–treated mice

B.

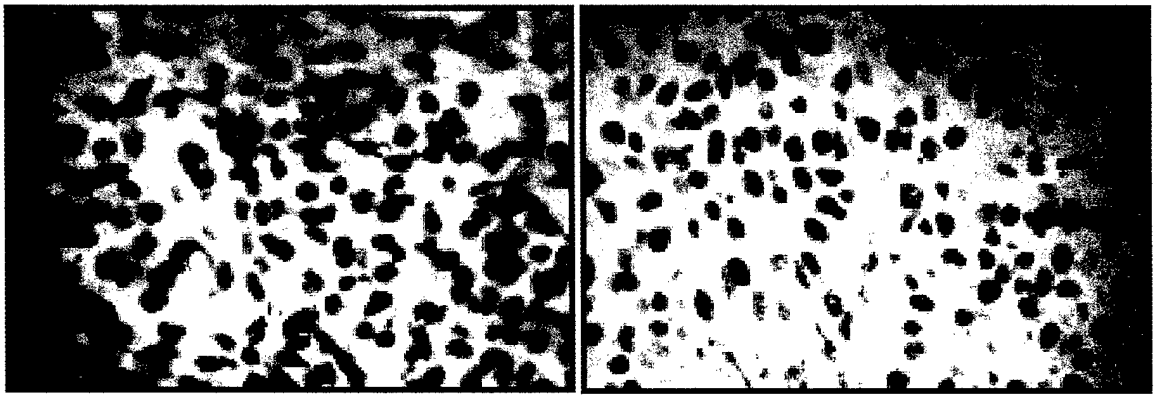

Figure 6